NANOPOROUS CONDUCTING HYDROGEL-BASED POINT OF CARE DEVICE FOR BREAST CANCER DETECTION

A major project dissertation submitted in partial fulfillment of the requirement

for the degree

of

Master of Technology

In

Biomedical Engineering

Submitted by

Ratan Kumar Chaudhary

Roll No. 2K15/BME/06

Under the supervision of

Prof. B. D. Malhotra

Department of Biotechnology
Delhi Technological University
Delhi-110042, India

DECLARATION

I, Ratan Kumar Chaudhary, hereby declare that the M. Tech. dissertation entitled "**Nanoporous conducting hydrogel based point of care device for breast cancer detection"** submitted in partial fulfilment of the requirement for the award of the degree of Master of Technology (Biomedical Engineering), Delhi Technological University (Formerly Delhi College of Engineering), is a record of original and independent research work done by me under supervision and guidance of **Prof. Bansi. D. Malhotra**, Department of Biotechnology, Delhi Technological University, Delhi. The information and data enclosed in the dissertation in original and has not formed the basis for the award of any degree/diploma or another similar title to any candidate of the university/institution.

Date:

Ratan Kumar Chaudhary
Roll No. 2K15/BME/06
M.Tech.(Biomedical Engineering)
Department of Biotechnology,
Delhi Technological University,
Shahbad Daulatpur,
Main Bawana Road,
Delhi – 110042, India

DELHI TECHNOLOGICAL UNIVERSITY

CERTIFICATE

This is to certify that the dissertation entitled "**Nanoporous conducting hydrogel based point of care device for breast cancer detection"** submitted by **Ratan Kumar Chaudhary (2K15/BME/06)** in the partial fulfilment of the requirements for the reward of the degree of Master of Technology in Biomedical Engineering, Department of Biotechnology, Delhi Technological University (Formerly Delhi College of Engineering), Delhi-110042 is an authentic record of the candidate's own work carried out by him under my guidance. The information and data enclosed in this thesis are original and has not been submitted elsewhere for honoring of any other degree or diploma.

Prof. Bansi D. Malhotra
(Project Mentor)
Department of Biotechnology
Delhi Technological University
Delhi- 110042

Prof. D. Kumar
(Co- Project Mentor &Head)
Department of Biotechnology
Delhi Technological University
Delhi- 110042

ACKNOWLEDGEMENT

I hereby express my profound sense of reverence of gratitude to my mentor Prof. B. D. Malhotra, Department of Biotechnology, Delhi Technological University, for his valuable guidance, congenial discussion, incessant help, calm, endurance, constructive criticism and constant encouragement throughout these investigations right from the imitation of work to the ship shaping of the project report.

I express my kind regards and gratitude to Vice-chancellor Yogesh Singh and Prof. D. Kumar, Head of Department (HOD), Department of Biotechnology, Delhi Technological University, Delhi for his interest and encouragement at various stages.

I am highly indebted to Ms. Shine Augustine, Dr. Saurabh Kumar, Dr. Suveen Kumar, and Mr. Ashish Kalkal for their guidance and constant supervision as well as for providing necessary information regarding the instruments and experiments and also for their support in completing the report.

I would also like to express my sincere thanks to Anas Saifi, Rahul Kandpal and Tarun Narayan for helping in lab work and their much-needed cooperation.

I am also thankful to all the staff members of the Department of Biotechnology, DTU; especially Mr. Chail Bihari, Mr. Jitendra Singh for providing necessary chemicals and maintaining a laboratory in good working conditions.

I have no word to express my deep sense of gratefulness and affection to all my family members and friends for their continuous love, support, encouragement, and of course persuasion to continue to study and understand the true value of education and the rewards of perseverance.

Last but not the least, thanks to all other who have not been mentioned by name but they have given invaluable help and encouragement.

Ratan Kumar Chaudhary
2K15/BME/06

CONTENTS

List of Abbreviations

Ab	Antibody
Ag	Antigen
APTES	3-Aminopropyl triethoxysilane
AgCi	Silver chloride
ITO	Indium tin oxide
BSA	Bovine serum albumin
CE	Counter electrode
CV	Cyclic voltammetry
DPV	Differential Pulse Voltammetry
EIS	Electrochemical impedance spectroscopy
DI	Deionized
GG	Guar gum
GGH	Guar gum hydrogel
ng	Nanogram
ml	Mililiter
JCPDS	Joint Committee on Powder Diffraction Standards
EDC	N'- ethyl -N- (3-dimethylaminopropyl) carbodiimide
NHS	N-hydroxysuccinimide
PBS	Phosphate buffer saline
$[Fe(CN)6]^{4-}$	Ferrocyanide
$[Fe(CN)6]^{3-}$	Ferricyanide
FTIR	Fourier transform infrared spectroscopy
XRD	X-ray diffraction
ELISA	Enzyme-linked immunosorbent assay
I_{pa}	Anodic peak current
I_{pc}	Cathodic peak potential
E_{pa}	Anodic peak potential
E_{pc}	Cathodic peak potential
R_{ct}	Charge transfer resistance (Nyquist diameter)
SEM	Scanning electron microscopy
E	Potential
fM	Femto Molar
M	Molar
HER-2	Human epidermal growth factor receptor- 2

List of Tables

LIST OF SCHEMES/FIGURES

CHAPTER 1

ABSTRACT

NANOPOROUS CONDUCTING HYDROGEL-BASED POINT OF CARE DEVICE FOR BREAST CANCER DETECTION

Ratan Kumar Chaudhary*

***Delhi Technological University, Delhi, India**

rtnkmr28@gmail.com

1. Abstract

A highly sensitive biosensor based on a guar gum hydrogel incorporated functionalized molybdenum trioxide nanoparticles electrode (APTES/MoO_3@GGH) was fabricated for the detection of breast cancer biomarker. One step Hydrothermal method was used for the synthesis of nanostructured molybdenum trioxide nanoparticle. Molybdenum trioxide nanoparticles were used to enhance the conductivity, immobilization and also retain the immunoactivity of the antibody on the electrode. Cyclic voltammetry, differential pulse voltammetry, and electrochemical impedance spectroscopy were used for characterization of various layers coated onto the APTES/MoO_3@GGH.The interactions of the antibody with different concentrations of antigen were also monitored via the change of current response.When we increase the concentration of HER-2 antigen the charge transfer resistance, also increases linearly. The electrochemical response studies of BSA/anti-HER-/MoO_3@GGH/ITO immunoelectrode reveal that this immunoelectrode can be used to measure HER-2 (breast cancer biomarker) concentration in serum samples, with a high sensitivity of 3.01 mA mL ng $^{-1}$, a linear detection range of 1 fg mL^{-1} - 10^3 ng mL^{-1}, limit of detection 0.132 ng mL-^{1}and stability of 4 weeks. The results showed that the prepared biosensor can be used for detection of HER2 present in serum samples of breast cancer patients.

CHAPTER 2

INTRODUCTION

2. Introduction

Hydrogels are one of many natural and synthetic polymers -based systems that embrace numerous biomedical applications. Hydrogels are crosslinked polymer networks that absorb and retain substantial amounts of water or biological fluids [1]. Due to their high water content, smartness, elastomeric nature, porosity soft and rubbery consistency, high permeability and they closely simulate natural living tissue because of their degree of flexibility makes unique hydrogel biomaterials [2,3]. The ability of hydrogels to imbibe water emerging from hydrophilic functional group joined to the polymeric backbone, while their resistance to dissolution emerges from crosslinks between network chains. The hydrophilicity of the network is due to the presence of hydrophilic groups such as -NH_2, -COOH, -OH, -$CONH_2$, -CONH -, and -SO_3. To increase the electrical conductivity of hydrogel, various nanomaterials can be embedded such as nanostructured metal oxides, the metal conducting polymers, carbon, etc. [4]. While considering its mechanical properties, they are characterized by the elastic modulus, viscoelasticity, tensile strength [5].

Hydrogels experience a significant volume phase transition or gel-sol phase transition because of certain physical and chemical stimuli. The physical stimuli, such as temperature, light intensity, pressure, electric or magnetic fields. While Chemical stimuli, such as ionic factors, chemical agents, and pH, will change the interactions between solvent and polymeric chains at the molecular level or between polymer chains [6]. The response of hydrogels to external stimuli is mainly determined by the nature of the monomer, pendant chains, and the degree of cross-linkage and charge density [7]. The magnitude of response is also directly proportional to the applied external stimuli. Because of their inherent property of biocompatibility and high water absorption capacity, they offer good opportunities such as wound dressing, drug delivery, agriculture, dental materials, implants, injectable polymeric

systems, ophthalmic applications, hybrid-type organs (encapsulated living cells), protein delivery systems or tissue engineering scaffolds.

Recently, Conducting polymer hydrogels been used as a biomatrix for the fabrication of biosensor. Nanostructured incorporated conducting polymer hydrogels retains their original structure but also acquire the characteristics of nanomaterials such as quantum effect, large surface area and particularly the 3D conducting network which help in the designing and making the novel biosensors.) Conducting Hydrogels also provide good processability, which can easily cast into a thin film and any different pattern as its gelation [8]. These synergistic effects together help in utilizing this matrix for the development of an electrochemical biosensor. A nanostructured conducting hydrogels-based biosensing platform for human metabolite detection is reported [9] for the detection of metabolite such as uric acid, cholesterol, and triglycerides. Biosensors demonstrate excellent sensing performance with a wide linear range (uric acid, 0.07−1 mM; cholesterol, 0.3−9 mM, and triglycerides, 0.2−5 mM), high sensitivity, low sensing limit, and rapid response time (∼3 s). Electrochemical biosensing platform using hydrogel was prepared from ferrocene modified amino acid as highly immobilization matrix reported [10] This biosensor was utilized
for the detection of glucose in blood samples with results comparable to those obtained from the hospital. Network nanostructured polypyrrole hydrogel/Au composites as enhanced electrochemical biosensing platform reported [11] Carcinoembryonic antigen (CEA) was used as a model protein. The proposed immunosensor exhibited a wide linear detection range from 1 fg mL^{-1} to 200 ng mL^{-1}, and an ultralow limit of detection of 0.16 fg mL^{-1} (S/N = 3), and it also possessed good selectivity

Breast cancer is an uncontrolled growth of cells that starts growing in the breast. Breast

cancer is the leading type of cancer in women, worldwide accounting for 25% of all cases [9]. Most cancer diagnosed among the women is Breast cancer. It is also the second leading cause of cancer death among women after lung cancer. Symptoms of breast cancer may include, a change in breast shape, a lump in the breast, fluid coming from the nipple, or a dimpling of the skin. In those with distant spread of the disease, there may be bone pain, shortness of breath, or yellow skin, swollen lymph nodes. HER2 is a protein that increases the growth of breast cancer cells. The overexpression of HER2 is observed in some of the breast cancer cases, and treatments using a monoclonal antibody to this molecule is now in progress, it is only useful in patients with excess receptor levels. In recent years, the clinical usefulness of determination of HER-2 levels in serum samples of breast cancer patients and available technologies for the detection of HER-2. Current diagnostic tests for HER2 involve the analysis of tumor cells for either amplification of the HER-2 gene using fluorescent in situ hybridization (FISH), or immunohistochemistry (IHC) to determine the expression of the receptor within the cell membrane. However, both FISH and IHC procedures are complicated, time-consuming and require specially trained personnel to carry out the corresponding multi-step procedures. To overcome this, the problem we have fabricated a biosensor.

The biosensor is a device that can sense the biological signals into electric signals. The biorecognition layer is one of the major components of the biosensor. The surface, on which this biorecognition layer is deposited, is also of pivotal role to obtain a highly sensitive and selective biosensor. Development of the biosensors is one of the primary practical tools to cover the various application such as including point-of-care testing, food safety, and processing home diagnostics, environmental monitoring, biomedicine, drug discovery, defense, and security. Biological recognition element consists of different structures like antibodies, enzymes, tissues or living cells but the main point is that the specificity toward one

analyte and zero response to other interferents. There are a different process for coupling the biomolecules with sensors including entrapment into a matrix, entrapment into membranes, covalent bonding or physical adsorption [7]. A highly sensitive impedimetric immunosensor based on a gold nanoparticles/multiwall carbon nanotube-ionic liquid electrode (AuNPs/MW-CILE) was developed for the determination of human epidermal growth factor receptor 2 (HER2) reported [13] linear range (10-110 ng mL^{-1}) and limit of detection (7.4 ng mL^{-1}).

Here we report results of the study relating to the fabrication of MoO_3 incorporated guar gum hydrogel-based electrochemical biosensors. In this work, we synthesize the hydrogel using guar gum which is a polysaccharide and nonionic consists of the sugars mannose and galactose. The backbone of guar gum which has a linear chain of β 1,4-linked mannose residues to which galactose residues are 1,6-linked at every second mannose forming short side-branches. It is a biodegradable, high solubility, high viscosity non-toxic, biocompatible, and low-cost materials. To prepare nanocomposite hydrogel, the MoO3 nanoparticles is functionalized with amine group by coating them with APTES. This nanocomposite based biosensor was used to detect breast cancer biomarker HER-2 in serum of breast cancer patients. The fabricated immunoelectrode gives fast response time, label free, low detection range, highly sensitive with an increased shelf life.We have developed the biosensors to detect breast cancer biomarker HER-2 present in serum using the electrochemical technique.

CHAPTER 3

LITERATURE REVIEW

3. Literature Review

3.1. Hydrogel

Hydrogel has shown unique properties due to this attracted considerable interest in the scientific research and various applications. The term hydrogel is a three-dimensional network structure obtained from a class of natural and synthetic polymers. Hydrogels have the ability to absorb and retain water arises from hydrophilic functional group attached to the polymeric backbone, while their resistance to dissolution arises from cross-links between network chains [14]. The hydrogel structure created by the hydrophilic groups or domains present in a polymeric network upon the hydration in an aqueous environment. Due Hydrogels show a swelling behavior instead of being dissolved in the aqueous surrounding environment as a consequence of the critical crosslink's present in the hydrogel structure [15]. Two main categories of crosslinks include i) chemical (tie-points and junctions) and ii) physical (entanglements or crystallites). The polymer chain is Crosslinks due to Vander Waals interactions, covalent bonds, hydrogen binding, or physical entanglements [15]. Natural polymers and their derivatives include (i) Anionic polymers: hyaluronic acid, alginic acid, pectin, carrageenan, chondroitin sulphate, dextrin sulphate. (ii) Cationic polymers: chitosan, polylysine (iii) Amphipathic polymers: collagen (and gelatine), carboxymethyl chitin, fibrin (iv) Neutral polymers: dextrin, agarose, pullulan. Synthetic polymers include PEG-PCL-PEG, PLA-PEG-PLA, etc. The benefits of the hydrogels are it can protect cells, Biocompatibility, it can also be injected in a whole, living organism as a liquid that then gels at body temperature[15].Timed release of medicines or nutrients, Excellent transport properties (such as nutrients to cells or cell products from cells), biodegradable or bioabsorbable and Easy to modify. These are the following limitations of the hydrogels are it shows low mechanical strength, not easy to handle, difficult to load with nutrients or drugs, non-adherent and difficult to sterilize.

Hydrogel technical features

These are the functional character of the hydrogel are

- The highest absorbency under load (AUL).
- The lowest soluble content and residual monomer.
- The lowest price.
- The desired rate of absorption (preferred particle porosity and size) depending on the requirement of the applications
- pH-neutrality after swelling in water.
- The highest absorption capacity in saline,
- Colorlessness, odorlessness, and absolutely non-toxic.
- Photostability
- The maximum biodegradability without formation of toxic species following the degradation.
- The highest stability and durability in the swelling environment and during the storage.

Guar Gum, either modified or unmodified is a very versatile and efficient natural polymer covering a large number of applications in various industries like food, pharmaceuticals, cosmetics, paper, textile, construction, beverages, oil & gas well drilling, mining, etc literature review.

Breast cancer following polyacrylamide hydrogel injection for breast augmentation A case reported [16]. The synthesized device was pH sensitive and was effective for colon-specific drug delivery. Cross-Linked Guar Gum Hydrogel Discs for Colon-Specific Delivery of Ibuprofen Formulation and In Vitro Evaluation was reported [17]. The fabricated hydrogel discs may, thus, prove to be beneficial as colon-specific drug delivery vehicles for poorly water-soluble drugs like ibuprofen. Gel-based microarrays in clinical diagnostics reported [18] Immobilization of molecular probes in 3D hydrogel elements provides some essential

advantages compared with conventional flat surfaces. The structure of the gel can be adapted for immobilization of virtually any biological molecules in a natural hydrophilic environment.

3.2. Applications of Hydrogels

Hydrogels is an important collection of resources with incredible purposes in engineering, biology, and pharmaceutical sciences. Polyelectrolyte hydrogels are mainly useful as they either carry or develop charges on the chain and bind with opposite-charged species to form complexes, which highlight their numerous applications in drug delivery, protein, peptide, pesticides nutrient, hormone, agriculture, horticulture, biotechnology, cell construction, pharmaceutical and biomedical applications [19]. Among the synthetic carriers, cationic polymers receive greater attention, because they can reduce large structures into smaller ones, and cover negative DNA charges, which are required for transfecting most types of cells, gene, antisense therapies and bile acid sequestrates, and for developing viral and nonviral vectors for DNA and oligonucleotide delivery. Hydrogels exhibit considerable volume changes in response to small changes in their surroundings, such as variations in the electric field, magnetic field, solvent, pH, ionic strength, and temperature.

3.2.1. Biomedical applications

Hydrogels copy the behaviour of human organs in response to changes in the environmental conditions such as pH, temperature, enzymes and electric field, which find applications in medical implants, prosthetic muscles or organs, robotic grippers, diagnostic devices to artificial muscles, detection of breast cancer, stabilization of bone implants, intimal thickening in animals and decreasing thrombosis, sensor technique, protein adhesion [19,20,21,22]. Hydrogels used in urinary catheters can prevent bacterial colonization on the surface, and provide a smooth and slippery surface to improve its biocompatibility [23].

3.3. Nanostructured metal oxides (NMOs)

Metal oxides is an important class of materials which are used in various fields, such as catalysis, transistors, energy storage and conversion, biomedicine and sensors. Nanostructured metal oxides have attracted a large amount of interest in recent years as immobilizing matrices for the development of the biosensor. A number of Nanostructured metal oxides (NMO) such as zirconium oxide (ZrO_2), titanium oxide (TiO_2), iron oxide ($Fe3O_4$), nickel oxide (NiO), aluminium oxide (Al_2O_3), magnesium oxide (MgO), molybdenum trioxide (MoO_3), copper oxide (CuO) show the interesting features like nano morphological, functional biocompatible, large surface area ,high surface to volume ratio, non-toxic, electrical, mechanical, optical and catalytic properties when their structural feature size is down to nanoscale.[24,25]. These materials also exhibit enhanced electron-transfer kinetics and strong adsorption capability, providing good environments for the immobilization of biomolecules and resulting in increase electron transfer and improved biosensing characteristics. Various morphologies of Nanostructured metal oxides have been obtained using a variety of methods, such as soft templating for the preparation of nanorods and nanofibers [26]. sol–gel methods for the production of three-dimensional (3D) ordered rough nanostructures [27,28], radio-frequency sputtering for rough nanostructures [29] and we have used hydrothermal method for the fabrication of molybdenum trioxide. These are the NMOs have been already reported to have significant applications in biosensors. Recently, the magnetic optical, and electrical properties of NMOs have been reported to be enhanced through the incorporation of nanoparticles of conducting or semiconducting materials such as carbon nanotubes, molybdenum, graphene, gold, and silver, as well as quantum dots of various semiconductors, have shown an advantage for improved the biosensor characteristics. It shows that the different application of an NMO may lead to the fabrication of new types of biosensing devices with enhanced signal amplification and coding strategies for bioaffinity assays and efficient electrical communication with redox biomolecules/ enzymes that may address future diagnostic or

detection needs. The unique properties of NMOs offer significant prospects for interfacing biological recognition events with electronic signal transduction and for designing a new generation of bioelectronics devices that may show new functions. The controlled preparation of an NMO is considered to play a important role in the development of biosensors. Efforts are being made to explore the prospects and future challenges of NMOs for the development of biosensing devices [30].

3.4. Biosensor

Biosensor is an innovative and powerful analytical device involving biological sensing element with a broad range of applications, such as food safety and processing, environmental monitoring, drug discovery, diagnosis, biomedicine, security, cancer detection, and defense. The first biosensor invented by Clark and Lyons (1962) to measure glucose in biological samples utilized the strategy of electrochemical detection of oxygen or hydrogen peroxide using immobilized glucose oxidase electrode [31]. Since then, significant progress has been made in the fields of technology and applications of biosensors with novel approaches involving electrochemistry, nanotechnology to bioelectronics. There are various technical strategies, adopted for developing biosensors to provide basic knowledge and present scientific scenario of biosensor technology. To demonstrate the performance of different biosensors evolved from the classical electrochemical to optical/visual, silica, glass, polymers and nanomaterials to improve the detection limit, response time, reproducibility, stability sensitivity, and selectivity. Biosensors provide a basis to understand technological improvement in the instrumentation involving complex high-throughput machines for quantitative biologists and semi-quantitative or portable qualitative device for non-specialist [31].

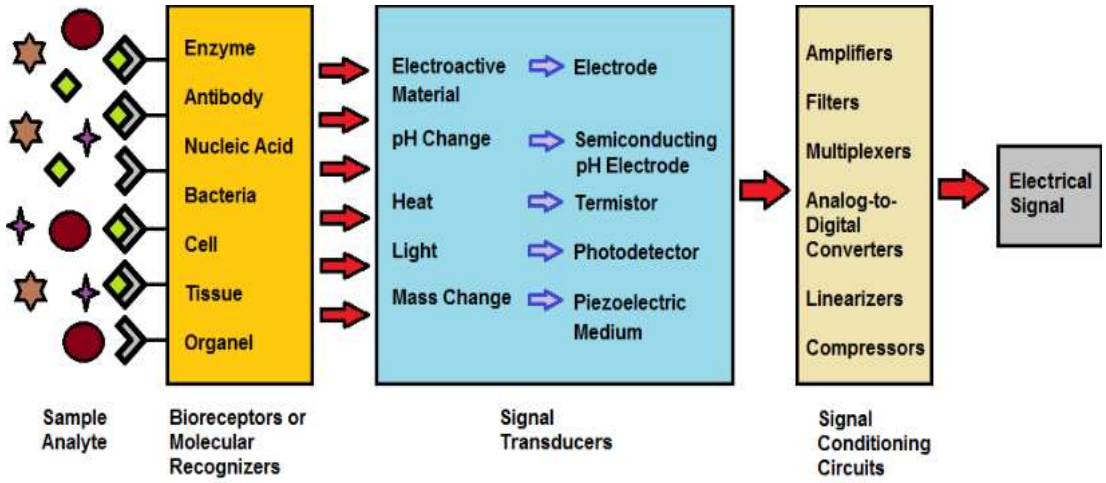

Figure 3.1: The basic function and structure of a biosensor.

There are different methods of attachment of biosensing elements to transducer unit are divided into the three generation [32].

First generation: The simplest approach to a biosensor where the normal product of the reaction diffuses on the surface of the transducer and causes the electrical response. These biosensors are designed by entrapping the biocatalyst in the membrane, which in turn is fixed on the surface of the transducer.

Second generation: In compare to the first generation it gives a better response. To achieve biosensors having improved response the use of redox mediators between reaction and transducer was introduced. In this generation, biosensors involve adsorption or covalent fixation of the biologically active component to the transducer surface and which allow the removal of a semi-permeable membrane.

Third generation: This is the novel biosensors in this bioreceptor is an integral part of the transducer itself. In this no redox mediators are used, Here response is caused by direct electron transfer between reaction and transducer.

3.4.1. Components of a biosensor

Biosensor can be classified into three important components: (a) Biological elements such as enzyme, antibody, microorganism, tissue, cell, nucleic acid etc. for the recognition of analyte known as bio-receptor (b) immobilization matrix such as nanomaterials, self-assembled monolayers and conducting polymers that are used for the immobilization of a biomolecule and (c) a transducer for conversion of the biological signal to a recognizable signal which may be electrical, optical or physical in nature. Bioreceptors along with transducer is also known as biosensor membrane.

3.4.1.1. Biomolecular recognition element

The definition of molecular recognition refers to the specific interaction between two or more molecules through noncovalent bonding such as π-π interactions, halogen bonding hydrogen bonding, metal coordination, hydrophobic forces, van der Waals forces, electrostatic and electromagnetic effects. The biomolecular recognition elements are as living organisms as the analytes that have been monitored using biosensors. Living organisms offer a variety of natural recognition elements such as antibodies, enzymes, nucleic acids, or even whole cells and viruses. Proteins are especially well-suited for highly selective recognition of other molecules. The most common recognition elements are used in biosensors are antibodies (Ab) and on the basis of their elective properties and the synthesis protocol they are classified as polyclonal, monoclonal or Recognition elements are crucial components of biosensors responsible for the recognition and capture of target molecules. Applying the basic principles

of biological recognition, we can create synthetic molecules with novel binding specificities (artificial binding proteins, aptamers/spiegel meres, peptide nucleic acids, etc.). These bio molecular recognition elements should have the ability to recognize biomarkers that are secreted in body fluids such as saliva, urine, blood etc. Among all these Blood is generally most commonly fluid used for the detection of biomarkers.

3.4.1.2. Immobilization Matrix

A prominent part of a biosensor is a matrix which is used for the Immobilization not only helps in forming the required close proximity between the biological molecules and the transducer, but also helps in stabilizing it for reuse. The biological molecules have been immobilized directly on the transducer or in the most cases, in membrane, which can be subsequently be mounted on the transducer. Biological molecules can be immobilized either through adsorption, entrapment, covalent binding, covalent binding, crosslinking or a combination of all these techniques. The characteristics of a favorable immobilizing matrix it should depend on a wide range of physiological temperature, ionic strength, pH and chemical composition. Cross-linking using bifunctional reagents like glutaraldehyde has been successfully used for the immobilization of cells. Covalent binding, a commonly used technique for the immobilization of enzymes and antibodies, has not been useful for the immobilization of cells. The covalent binding of a biomolecule involves the formation of covalent bonds between biomolecules and support matrix. In a covalent binding, biomolecule and matrix bind with the help of functional group such as $–NH_2$, -SH, -OH, etc. that are present on them. This method has been employed to improve uniformity, density, and distribution of the bound proteins, as well as reproducibility on the surfaces. In the present work, we have used APTES/MoO3@GGH nanocomposite hydrogel as immobilization matrix for fabricating the biosensor for breast cancer detection.

3.4.1.3. Transducer

A transducer is a device which converts one form of the signal into another form. In the biosensor, the transducer converts the biological signal received from biochemical activity between a biological component and an analyte into an electrical signal. Analytical characteristics of the biosensor, such as detection limit, signal stability, reproducibility, and selectivity are determined by transducer efficiency. Different types of biosensors are classified as an electrochemical biosensor, optical biosensor, piezoelectric biosensors, pyroelectric biosensor, electronic biosensor and gravimetric biosensor.

Potentiometric biosensor: In this kinds of biosensors changes, the concentration of ionic is measured by the ion-selective electrodes in this pH electrodes are commonly used**.** This biosensor measures the potential at the working electrode on reference electrode and then measures the charge generated through selective biomolecular binding at the electrode surface.

Amperometric biosensor: The biosensors are based on the electrons movement, change in electronic current determination as a redox reaction occurs between the biomolecular species present on the working electrode. A normal voltage passes through the electrodes to analyze. These biosensors show cost effectiveness, high sensitive, and rapidity.

Conductometric Biosensor: This device consists of two noble metal electrodes, which are immersed in the solution and the conductance is measured. Some enzymatic reactions convert neutral substrates into charged products, causing a change in the conductance of the medium. Although this transducer is not in widespread use, the technique is routinely used to measure salinity of marine environments. The main advantages of electrochemical biosensors are simplicity, fast response time and low cost.

Piezoelectric biosensors: The piezoelectric biosensor is a device made of Piezoelectric crystals, and the characteristic frequencies are trembling with the crystals of negative and positive charge, the resonance frequency changes during biomolecular interaction which can

be converted into an electrical signal proportional to the amount of biomolecules species present. The piezoelectric biosensor not only offers ease of use, real-time output but also provide a wide pH range for working [33].

Calorimetric biosensors: The calorimetric biosensors are based on the heat generated during the biochemical reaction between analyte and sensing biomolecule. Most of the heat evolved during a chemical reaction is lost into the surrounding medium without being detected; this biosensor is not sensitive enough to produce accurate results.

Optical biosensor: Optical biosensors are the devices based on the optical principle that can measure light produced through the biochemical reaction between the two products. Optical biosensors that exploit fluorescence, absorption, luminescence, and Raman scattering and refracting index are a powerful alternatives to conventional analytical technique. These biosensors provide fast, real-time and high-frequency monitoring without time-consuming and sample preparation step.

Electrochemical biosensor: An electrochemical biosensor is a biosensor with an electrochemical transducer to analyze the content of a biological sample due to the direct conversion of a biological event to electrical signal. It is considered a chemically modified electrode (CME). Since electronic conducting, semiconducting or ionic conducting material are coated with a biochemical film. A biosensor is an integrated receptor-transducer device, which is capable of providing selective quantitative or semi-quantitative analytical information using a biological recognition element. Chemical sensors, which incorporate a non-biological specificity-conferring part or receptor, although used for monitoring biological processes, as the in vivo pH or oxygen sensors are not biosensors.

A number of different electroanalytical techniques is used to study the electrochemical characteristics of the fabricated immunoelectrodes, and to analyze their response to Breast cancer biomarker . Some of these electroanalytical techniques are

Cyclic Voltammetry (CV): Cyclic Voltammetry (CV) is an electrochemical technique which measures the current that develops in an electrochemical cell under conditions where voltage is in excess of that predicted by the Nernst equation. Cyclic Voltammetry can be used to study qualitative information about electrochemical processes under various conditions, such as the presence of intermediates in oxidation-reduction reactions, the reversibility of a reaction.

Differential Pulse Voltammetry (DPV): In this technique where the cell current is measured as a function of time and as a function of the potential between the indicator and reference electrodes. The potential is varied using pulses of increasing amplitude and the current is sampled before and after each voltage pulse. The height of the peak obtained in the differential pulse voltammogram is proportional to the concentration of the analytes.

Electrochemical Impedance Spectroscopy (EIS): Electrochemical impedance spectroscopy (EIS) is a powerful tool to measure the flow of ions through solution, interface and coatings, for studying interfacial properties of the surface-modified electrodes. The EIS technique is commonly applied for the investigations of electrode kinetics, adsorption behaviour and interaction of biomolecule with the electrode surface. Electrochemical impedance is usually measured by applying an AC potential of different frequencies to an electrochemical cell and measuring the current through the cell.

3.5. Cancer

Cancer can be defined as a disease in which a group of abnormal cells grows uncontrollably by disregarding the normal rules of cells division [34]. Mainly, human cells grow and divide to form new cells as the body needs them. When cells become damaged or grow old, they die, and new cells take their place. Many cancers form solid tumors as well as do not forms the solid tumors, which are masses of tissue or blood. Malignant tumors which can spread in the

body or penetrate the nearby tissues, For example, breast cancer that spreads to and forms a metastatic tumor in the lung is metastatic breast cancer, not lung cancer, Metastasis is the main causes of death related to cancer almost 90% [35]. Benign tumors do not spread into the body or penetrate the tissues, unlike malignant tumors. The genetic changes that contribute to cancer tend to affect three main types of genes proto-oncogenes, tumor suppressor genes, and DNA repair genes. Over 200 types of cancer affect the human. These types of cancer are commonly named depending on the origin.

3.5.1. Breast cancer

Breast cancer is an uncontrolled growth of the cell in the breast. The most common breast cancer is ductal carcinoma which starts in the cells of the lobules, which are the milk-producing ducts, the passages that drain milk from the lobules to the nipple. Less common, breast cancer can begin in the stromal tissues, which include the fatty and fibrous connective tissues of the breast. Invasive breast cancer is breast cancer that has spread from where it started in the breast ducts or lobules to surrounding healthy tissue [36]. Breast cancer mostly occurs in women, but it also occurs in men too.As a woman gets older, the risk of developing breast cancer also increases gradually. All women at the age of 40 and older are at risk for breast cancer. This disease is uncommon in women under the age of 35. However, most of the breast cancers occur in women over the age of 50, and the risk is mainly growing for women over 60 years old.

The following factors place a woman at high risk for breast cancer:

- **Personal history of breast cancer:** Chance of getting breast cancer again is high in those women who have to face it earlier.

- **Genetic alterations:** Changes occur in some genes (BRCA2, BRCA1, and others) make women more vulnerable to breast cancer. Many women in their family have had the disease; gene testing can show whether a woman has particular genetic changes known to increase the chances of getting breast cancer.
- **Family history:**A woman's risk of growing breast cancer is high if her, sister, daughter, mother, or more than two close relatives, such as cousins, have a history of breast cancer, particularly at a young age.
- **Certain breast changes:** Having a diagnosis of lobular carcinoma in situ (LCIS) or atypical hyperplasia or two or more than two breast biopsies for other benign conditions may increase the risk of developing breast cancer in woman's risk.

Breast cancer include some other factors associated which increase the risk

- **The density of Breast:** The age of women is 45 or above whose mammograms show at least 75 percent dense tissue are at high risk of developing the breast cancer. The density of breast contains many ligaments and glands, which makes breast tumors difficult to view and the dense tissue itself is related with high chances of growing breast cancer.
- **Radiation therapy:** During the childhood Women whose breasts were exposed to radiation mainly those who were treated with radiation for Hodgkin's lymphoma are at high risk of growing breast cancer throughout their lives.
- **Late childbearing:** Women who had their children at a younger age have less chance of developing breast cancer than women who had their first child after the age of 30 or older. Studies also show that most women who develop breast cancer have none of the risk factors mentioned above, other than the risk that comes with growing older. Also, most women with known risk factors do not get breast cancer

3.6. Conventional detection methods for breast cancer

In recent years, there are numerous techniques has been identified to improve the prognosis and diagnosis such as FISH, IHC, biopsy, MRI, etc.

Biopsy: A biopsy is a small surgery done to remove a small sample of tissue from an area of concern in the Breast. The tissue sample is then examined by a pathologist under the microscope to look for abnormal cells are present or not. Biopsy possess a significant number of limitations the amount of tissue obtained from a biopsy may not be enough, and the biopsy may have to be repeated Surgical biopsy requires the application of local anesthesia and can be particularly uncomfortable and may cause to trauma. This method is invasive, time-consuming, expensive and require highly skilled personnel

Mammography: Mammography is especially the only extensively used imaging technique for breast cancer screening.It is the process of using low X-ray. It is useful in reducing breast cancer mortality rates in several studies. But the success of any screening program of asymptomatic women depends on the detection of subtle and small lesions. Advancements over many years in the quality performance and the reporting of mammography studies are the most significant advances in breast imaging [37].

Magnetic resonance imaging (MRI): MRI is a powerful imaging technique that uses strong radio waves, magnetic fields and field gradients to produced detailed images of the organs inside the body. It does not involve any radiation exposure because MRI does not use X-ray. MRI has remarkable sensitivity for the detection of breast cancer and relates cancers that are entirely unknown on conventional imaging. Reported sensitivities for invasive cancers using dynamic intravenous gadolinium-based contrast agents are consistently greater than 90% [37]. Dynamic contrast-enhanced breast MRI is clinically used to produce volumetric three

dimensional anatomical information and physiological process that is demonstrative of increased vascular density and vascular permeability changes associated with angiogenesis . It's cost is high, requires injection of a contrast agent for functional imaging and also needed a longer time to scan.

Fluorescence in situ hybridization (FISH): FISH testing is performed on breast cancer tissue removed during the biopsy to see whether the cells have extra copies of the HER-2 gene. The more copies of the HER-2 gene that are present, the more HER-2 receptors the cells have [38]. These HER-2 receptors receive signals that increase the growth of breast cancer cells. Normally, the FISH test is not extensively available as another method of HER-2 testing, called ImmunoHistoChemistry, or IHC. However, the FISH technique is considered as the more accurate. In most of the cases, the FISH test will be performed after the IHC test if IHC results don't indicate whether the cells are HER2- negative or positive. Research has shown that some HER2 test results may be the wrong, i.e. FISH test generally not recommend.

Immunohistochemistry (IHC): IHC refers to the process of primarily imaging antigens (e.g. proteins) in cells of a tissue section by exploiting the principle of antibodies binding specifically to antigens in biological tissues [39]. ImmunoHistoChemistry is a unique staining process performed on frozen or fresh breast cancer tissue removed during the biopsy. IHC is used to identify whether the cancer cells have HER-2 receptors and hormone receptors on their surface. This information plays a crucial role in treatment planning. IHC is the most frequently used test to check if a tumor has a high quantity of the HER-2 receptor protein on the surface of the cancer cells with a large quantity of HER-2 receptors due to this cells receive too many signals then it will grow and divide. Some research shows that Res HER2 test results may be wrong because different labs have various methods for classifying positive and negative HER2 status.

CHAPTER 4

MATERIALS AND METHODS

4. Material and methods

4.1. Chemicals and reagents

Guar gum powder was procured from chemical drug house pvt. Ltd. Sodium borohydride ($NaBH_4$), Ethylenediamine ($C_2H_8N_2$), Sodium Molybdate dihydrate ($Na_2MoO_4.2H_2O$), Nitric acid (HNO_3), PH strip and Whatman filter paper were purchased from sigma-Aldrich Chemicals.1-(3-(dimethylamonia)-propyl)-3-ethlcarbodiimide hydrochloride (EDC) [$C_8H_{17}N_3$] of AR grade were purchased from Sigma-Aldrich. Sodium Monophosphate [NaH_2PO_4], Sodium Diphosphate dihydrate [$Na_2PO_4.2H_2O$], N-hydroxysuccinimide (NHS) [C4H5NO3], Potassium ferricyanide {$K_3[Fe(CN)_6]$} and Potassium ferrocyanide {$K_4[Fe(CN)_6]3H_2O$} were procured from Fisher Scientific. All chemicals were of analytical grade and were used without any further purification. Phosphate buffer saline (PBS) was prepared using $Na_2PO_4.2H_2O$ (0.05 mol L^{-1}) and NaH_2PO_4 (0.05 mol L^{-1}) of pH 7.4 Fresh PBS was prepared using Milli-Q water having a resistivity of 18 MΩ cm at 4 ^{o}C. The HER-2, and anti-HER- 2 were obtained from Ray Biotech, Inc., India.

4.2. EXPERIMENT

4.2.1. Hydrogel Synthesis: 1 g of guar gum is dissolved in 250 ml of distilled water and continuously stirred to get a Homogeneous solution. 25 ml of Ethylenediamine is added to the guar gum solution which is act as tetra Initiator and stirred it for at least 12 hours at room temperature. Then add 50 ml of NaBH4 solution 5% (W/V) which is act as a crosslinker to the reaction mixture. This was precipitation using acetone [40] . The precipitate obtained was washed with acetone and Filter by Whatman Paper and kept for drying at 55˚C for 4-5 hours

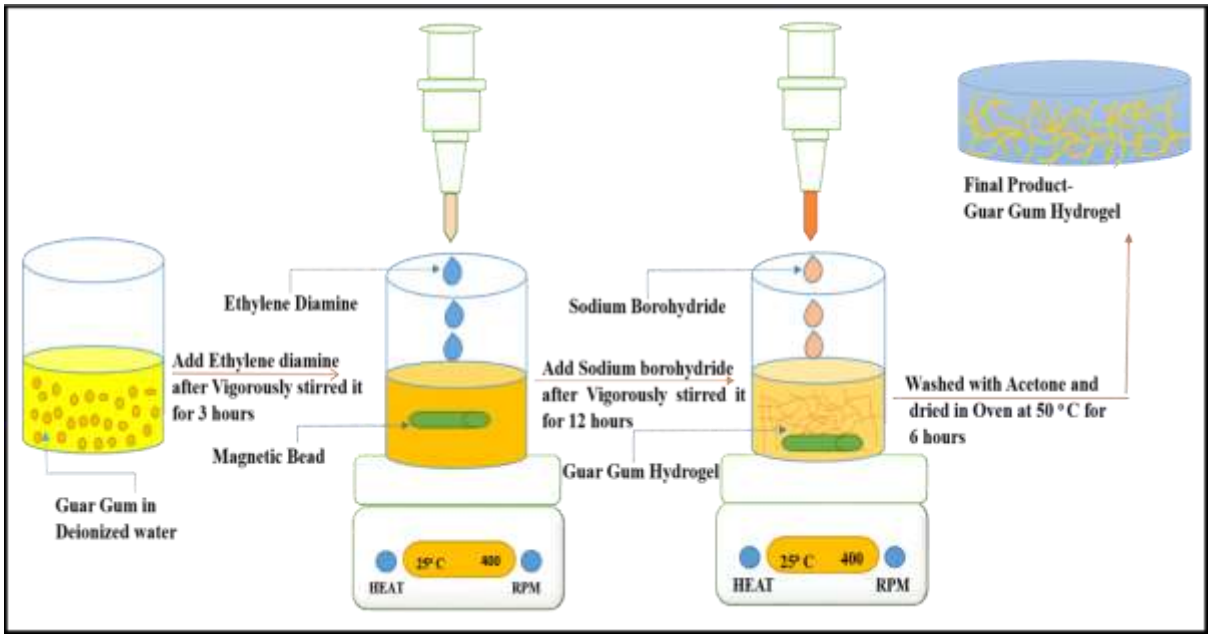

Scheme 4.1: Steps for the Synthesis of Guar Gum Hydrogel

4.2.2. Nanoparticle synthesis: We take 0.2 M Sodium Molybdate dehydrate added to the 10 ml of Distilled water. After vigorous stirring for 45 min, the solution becomes colorless and then add 5 ml of concentrated HNO_3 was introduced into the solution and continuously stirred at room temperature for two h. Mixer solution pH is 1 and color become pale yellow. The mixed solution was transferred into a Teflon vessel and placed in a stainless steel tank sealed and maintained at temperatures (T = 170 ◦C) for 18 hours put in an oven. The obtained precipitates were separated by centrifugation, washed with distilled water and ethanol and finally dried in an oven at 70 ˚C for 12 hours. Mortar pestle has been used to crush the product into powder form for further characterization.

4.2.3. Functionalization of Molybdenum trioxide Nanoparticles: 100 mg of MoO_3 nanoparticles was added to 20 ml of isopropanol and stirred it to obtain a highly dispersed suspension. Next, add 200µl of 98% APTES and also add 2 ml of Distilled water was mixed and continuously stirred at 300 rpm for 48h at room temperature (25 ^{o} C). To remove the

unbounded APTES, the suspension was centrifuged and washed thoroughly with deionized water and ethanol, finally dried in an oven at 60 ^{o}C for 18 h.

4.2.4. Composite of APTES/MoO_3 and GGH: Composite is defined as a combination of two altogether different types of materials was thought to generate not only structural diversity but also the most of the property enhancements. Such property improvements were the primary focus of research on hydrogel-nanoparticle composite materials that resulted in improved mechanical strength, electrical conductivity. Functionalised MoO_3 nanoparticle hydrogel composite made of molybdenum trioxide to enhanced the electric conductivity. For example, recently reported silica nanoparticle-hydrogel composite made of silica nanoparticles and modified polyethylene glycol demonstrated remarkable improvements in tissue adhesive property, mechanical stiffness and bioactivity compared to hydrogel without nanoparticles. Similarly, significant changes in mechanical property and thermal response were observed in poly-N -isopropylamide hydrogels when gold nanoparticles immobilized in the gel. The advantages of the combination of two different materials nanoparticle and hydrogels lead to promising materials with different properties absent in the individual materials. This particular feature has propel more research activity at the interface of nanoparticle-hydrogel composites looking forward to various applications over the past many years.

4.2.5. Fabrication of immunoelectrode: APTES functionalized MoO_3@GGH was deposited onto the prehydrolyzed ITO electrode via drop cast method. Prior to deposition, a colloidal suspension containing 6 mg, 5 mg of APTES/MoO_3 , and 1 mg of GGH was prepared in 6 mL of deionized water followed by ultrasonication. An optimized surface area of the APTES/MoO_3@GGH/ITO electrodes was determined to be 0.25 cm^2. The as-prepared electrode was dried in the oven at 60 ^{o}C for 45 minutes. After that Immobilization of anti-HER-2 over APTES/MoO_3@GGH/ITO Electrode .The anti-HER-2 solution (50 μg mL^{-1}) was prepared in PBS (pH = 7.0). 15 μL of anti-HER-2 was mixed with 7.5 μL of 0.4 M EDC

(activating agent) and 7.5 µL of 0.1 M NHS (coupling agent). Subsequently, this solution (30 µL) was uniformly spread onto APTES/MoO_3@GGH/ITO electrode by drop-casting. The electrode was kept at room temperature (25 °C) for 10-15 minutes and stored in fridge at 4 ^{o}C after electrode dried then followed by washing with PBS to remove any unbound antibody molecules. The -COOH group of anti-HER-2 can be covalently bound with -NH 2 terminal of APTES via strong amide bond (OC-NH). Then bovine serum albumin (BSA = 1 mg mL^{-1}) was used for blocking the nonspecific active sites of the electrode. The BSA/anti-HER-2/ APTES/MoO_3@GGH/ITO immunoelectrode was stored at 4 °C when not in use. Schematic 4.2 shows a step-wise fabrication process of the BSA/anti-HER2/APTES/MoO_3@GGH/ITO /ITO immunosensor along with the biochemical reaction.

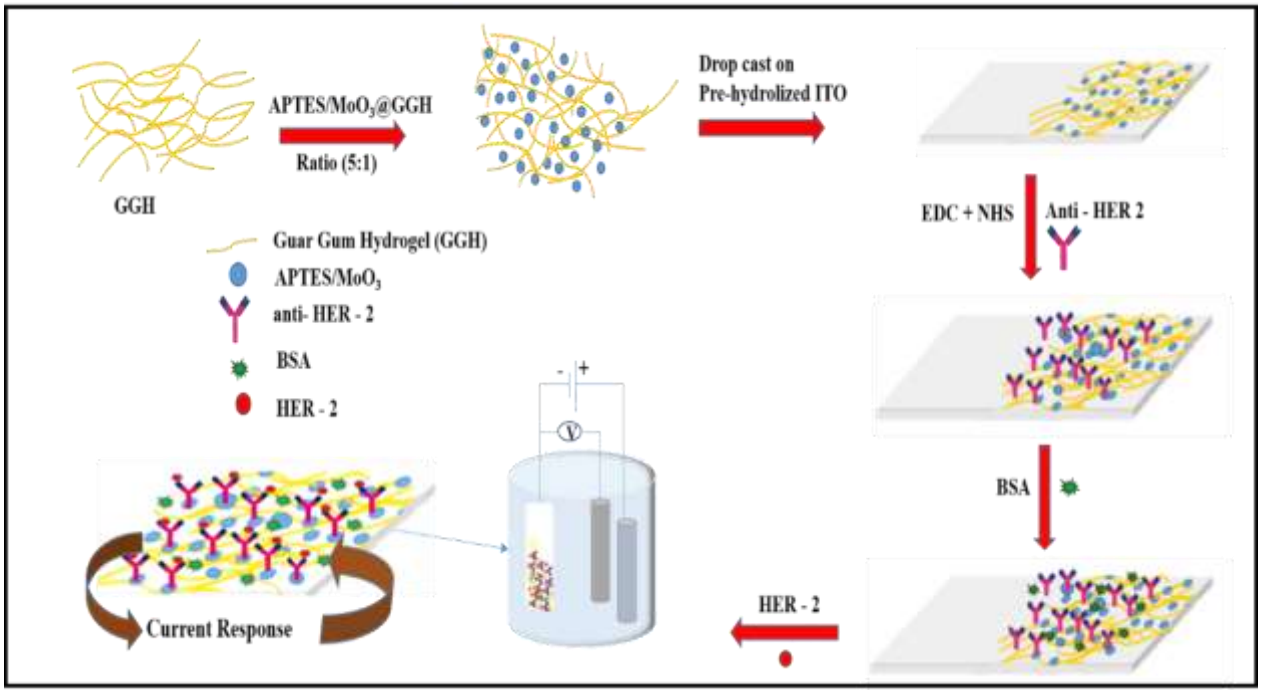

Scheme 4.2: Fabrication steps the of biosensing platform of BSA/anti-HER-2/APTES/MoO_3/GGH/ITO for detection of Breast cancer.

4.2.6. A collection of Serum Samples of breast cancer patients: The serum samples of breast cancer patient were collected from Rajiv Gandhi Cancer Institute and Research Centre, Delhi (India). All serum samples were obtained under a protocol certified by Rajiv Gandhi Cancer Institute, and Research Center Institutional Review Board (R.No. RGCIRC/IRB/60/2014) and written consent taken from the patients. Ethical approval of the Institutional Ethical and Biosafety Committee, DTU (R. No. BT/IEBC/2014/714) was also obtained. Samples were obtained, processed and stored under similar conditions. The unstimulated whole serum was collected from patients diagnosed with breast cancer. The collected serum was obtained in a sterilized tube and stored at -20 °C until further use.

4.2.7. Quantification of HER-2 present in serum of breast cancer: Enzyme-linked immunosorbent assay test (ELISA) is used for the quantification of HER-2 in the serum sample of four breast cancer patients. Double sandwich ELISA method was used in which anti-HER-2 precoated microtiter 96 well plate were used. In triplicate, Both the patient and standard samples were used. After performing all the steps, the colorimetric reaction occurred, and the absorbance was recorded at 450 nm in ELISA plate reader. A series of the HER-2 concentration of serum samples has been used to confirm the electrochemical response of the fabricated biosensor. It can be seen that a viable correlation exists between the magnitude of the cyclic voltammetry current response of the fabricated or developed immunoelectrode in the presence of (i) HER-2 concentration in serum samples determined by ELISA and (ii) Standard concentration of HER-2.The results obtained exhibit acceptable %RSD (relative standard deviation) indicating the high accuracy of the fabricated biosensor.

CHAPTER 5

INSTRUMENTATIONS

5. Instrumentations

5.1. Fourier Transform-Infrared Spectroscopy (FTIR): The Infrared source region is (12800 - 10 cm^{-1}) and it can be divided into three regions are near-infrared region (12800 - 4000 cm^{-1}), mid-infrared region (4000 - 200 cm^{-1}) and far-infrared region (200 - 10 cm^{-1}). Infrared absorption spectroscopy is the technique which used to determine the structures of molecules with the molecules' and also checks the function group in the chemical compound. The infrared spectrum is a molecular vibrational spectrum. When exposed to infrared radiation, sample molecules selectively absorb radiation of particular wavelengths which causes the change of dipole moment of sample molecules [41] (.). Accordingly, the vibrational energy levels of sample molecules transfer from ground state to excited state. The vibrational energy gap determines the frequency of the absorption peak. The number of absorption peaks is related to the number of vibrational freedom of the molecule. The intensity of absorption peaks is related to the change of dipole moment and the possibility of the transition of energy levels. Hence, by analyzing the infrared spectrum, one can readily obtain sufficient structure information of a molecule.The most commonly used region for infrared absorption spectroscopy is mid-infrared region 4000 ~ 400 cm^{-1} because the absorption radiation of most inorganic ions and organic compounds is within this region. In this work, we have conducted the FT-IR of GGH, APTES/MoO3, and APTES/MoO3@GGH. Wavenumber is the reciprocal of the wavelength. The intensity can be represented as the percentage of light transmittance at each wavenumber.

Precautions:

(i) Before starting the experiment, we should use nitrogen gas into the FT-IR chamber to prevent the interactions due to Co_2 and water.

(ii) Samples will be solid, liquid and gas form.

(iii) We mixed the Kbr and samples to prepare the pallet in such a way to light source pass through it. Samples and Kbr in the ratio 1: 200

Figure 5.1: Perkin Elmer FT- IR spectroscopy instrument

5.2. Ultraviolet–Visible Spectrophotometer: The ultraviolet–visible spectrophotometer consists of a light source, a wavelength selector, sample holder, a detector and signal processor. The light source is commonly used as a deuterium lamp or hydrogen at low pressure which releases electromagnetic radiation in the ultraviolet region of the spectrum. A second light source, a tungsten lamp, is commonly used for wavelengths in the visible region of the spectrum.We are using Perkin Elmer double-beam instrument, the light flow from the light source is split into two beams, one is the reference beam, and another is the sample beam. When there is no sample cell in the reference beam, the detected light is taken to be equal to the intensity of light entering the sample. The sample cell must be constructed of a material that is transparent to the electromagnetic radiation being used in the experiment.

Most organic molecules and functional groups are transparent in the portions of the electromagnetic spectrum in the ultraviolet (UV) and visible (VIS) regions.

whereas the wavelengths range of UV and VIS is from 190 nm to 800 nm. Consequently, absorption spectroscopy is of limited utility in this range of wavelengths. However, in some cases, we can derive useful information from these regions of the spectrum.)The complete range of the UV-Vis is from 190 nm to 3000 nm [42]. When continuous radiation or light source passes through a transparent material, a portion of the radiation may be absorbed. If that happen, the residual radiation, when it is passed through a prism, yields a spectrum with gaps in it, called an absorption spectrum. As a result of energy absorption, atoms or molecules pass from a state of low energy (the initial, or ground state) to a state of higher energy (the excited state). The electromagnetic radiation that is absorbed has energy exactly equal to the energy difference between the excited and ground states. In the case of ultraviolet and visible spectroscopy, the transitions that result in the absorption of electromagnetic radiation in this region of the spectrum are transitions between electronic energy levels The cuvettes for the sample, and reference solution must be transparent to the radiation which will pass through them. For the measurements in the UV region of the spectrum, Quartz, silica cuvettes are used because it does not have to absorb radiation in this region. However, glass and plastic cannot be used because they absorb ultraviolet light. These sample cells are also transparent in the visible region. For spectra in the visible range of the spectrum, cells composed of glass or plastic are commonly suitable. Silicate glasses can be used for the fabrication of cuvettes for use between 350 and 3000 nm. A modern improvement on the traditional spectrophotometer is the diode-array spectrophotometer. A diode array consists of a series of photodiode detectors positioned side by side on a silicon crystal. Each diode is designed to record a narrow band of the spectrum. The diodes are connected so that the entire spectrum is recorded at once. This type of detector has no moving parts and can record spectra very quickly. Furthermore, its output can be passed to a computer, which can process the information and provide a variety of useful output formats.

Precautions:

Sample solution should be transparent to pass the light source.

Figure 5.2: LAMBDA 950 UV-VIS spectrophotometer from Perkin Elmer

5.3. X-ray diffraction (XRD): X-ray diffraction (XRD) is perhaps the most commonly used X-ray based analytical tool for characterizing the substance. The sample is used in a powder form, consisting of fine particles of crystalline material to be studied. The term powder means that the crystalline domains are randomly oriented in the sample. Therefore when the 2-D diffraction pattern indicated, shows concentric rings of scattering peaks corresponding to the various d spacings in the crystal lattice. The intensities and positions of the peaks are used for recognizing the underlying phase(or structure) of the substance [43]. This structure recognition is necessary because the material properties rely heavily on the structure. The three-dimensional structure of crystalline materials defined by uniform, repeating planes of atoms that form a crystal lattice. When a focused X-ray beam interacts with these planes of atoms, a fragment of the beam is transmitted, and also some fragment is absorbed by the sample, the fragment is refracted and scattered, and the fragment is diffracted. Diffraction of an X-ray beam

by a crystalline solid is analogous to diffraction of light by droplets of water, producing the familiar rainbow. X-rays are diffracted by each mineral differently, depending on what atoms make up the crystal lattice and how these atoms are arranged. When a beam targets a sample and is diffracted, we can calculate the distances between the planes of the atoms that compose the sample applying the Bragg's Law, named after William. Lawrence Bragg, who first proposed it in 1921. Bragg's Law is $2dsin\theta = n\lambda$, where the integer n is the diffracted beam, λ is the wavelength of the incident X-ray radiation, d is the distance between adjacent planes of atoms (the d-spacings), and is the angle of incidence of the X-ray beam. In X-ray powder diffractometry, X-rays beam are generated within a sealed tube that is under vacuum. A current is applied that heats a filament within the tube; the higher the current, the greater the number of electrons emitted from the filament. This generation of electrons is analogous to the production of electrons in a television picture tube. A high voltage, typically 15-60 kilovolts, is applied within the tube. This high voltage accelerates the electrons, which then hit a target, commonly made of copper. When these electrons hit the target, X-rays are produced. The wavelength of these X-rays is characteristic of that target. These X-rays are collimated and directed onto the sample, which has been ground to a fine powder (typically to produce particle sizes of less than 10 microns). A detector detects the X-ray signal; the signal is then processed either by a microprocessor or electronically, converting the signal to a count rate. Changing the angle between the X-ray source, the sample, and the detector at a controlled rate between preset limits is an X-ray scan. Applications XRD analysis has a broad range of applications in material science, chemistry, geology, environmental science, forensic science, and the pharmaceutical industry for characterizing materials. Amorphous materials are readily recognized by the absence of peaks in an XRD chart. This method is used for studying particles in liquid suspensions or polycrystalline solids. Other applications of XRD analysis include determination of phase transitions in a given substance, semi-quantitative determination of

phases present in a sample, measurement of crystallite size particularly in nanomaterials. We have used the XRD to study crystalline structure of the materials GGH, MoO3, MoO3@GGH

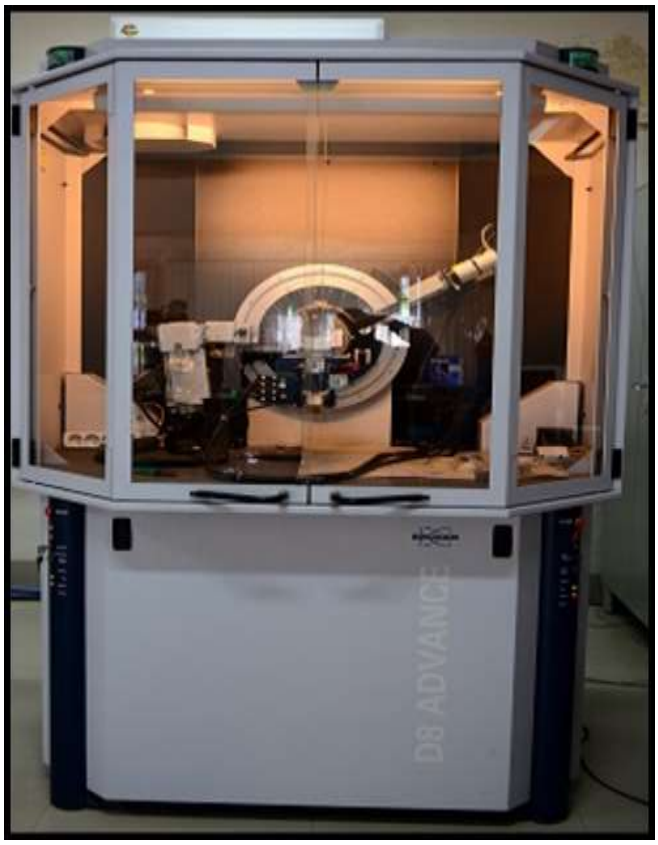

Figure 5.3: Bruker D-8 Advance XRD instrument.

5.4. Scanning electron microscopy: The scanning electron microscope (SEM) uses a targeted beam of high-energy electrons to generate a variety of signals at the surface of solid materials [44]. The signals that derive from interactions between sample and electron gives details about the sample including external morphology (texture, crystalline structure, chemical composition, a and orientation of materials making up the sample. In most of the applications, information is collected over a selected portion of the surface of the sample; SEM provides the 3-dimensional image that displays spatial variations in the properties. The approximate range of areas are 1 cm to 5 microns in width can be imaged in a scanning mode using conventional SEM techniques (magnification ranging from 20X to 30,000X, the spatial resolution of 50 to

100 nm). We can also perform the analysis of the sample at the particular point using SEM. This approach is necessary for the qualitatively or semi-quantitatively determining chemical compositions (using EDS), crystalline structure, and crystal orientations (using EBSD). We study the morphological analysis of the synthesized GGH, APTES/MoO3@GGH, anti-HER-2/APTES/MoO3@GGH electrode

Figure 5.4: Scanning electron microscopy instrument

5.5. Electrochemical Analyzer : Electrochemistry is an analytical technique that is used to measure the potential, charge or current to characterize chemical reactivity of an analyte or to determine the analyte concentration. Electrochemical techniques develop the relationship between the changes of an electrical signal to an electrochemical signal at an electrode surface; reaction occurs on the electrode surface it gives the information in potential or current [45]. Here, we are using three electrode system working electrode (WE), reference electrode (RE) and the counter electrode or auxiliary electrode (CE). WE are using platinum as a counter electrode which is an inert material, and it does not involve in the electrochemical reaction.

Because the current is flowing between the CE and the WE, CE total surface area must be higher than WE so that it will not be a limiting factor in the kinetics of the electrochemical process under investigation. Ag/Agcl used as a reference electrode which is a stable and well-known electrode potential, and it is used as a point of reference in the electrochemical cell for the potential control and measurement. The high stability of the reference electrode potential is reached by employing a redox system with constant (buffered or saturated) concentrations of each participant of the redox reaction. Furthermore, the current flow through the reference electrode is kept ideally zero which is achieved by using the CE to close the current circuit in the cell together with a very high input impedance on the electrometer. Indium tin oxide which is inert materials used as a working electrode in an electrochemical system on which the reaction will occur. The variation in shape and size of the working electrode and it depends on the application.

In the potentiostat mode, which correctly controls the potential of the Counter Electrode (CE) against the Working Electrode (WE) then the potential difference between the working electrode (WE) and the Reference Electrode (RE) is well defined, and correspond to the value specified by the user. In the galvanostatic mode, the current flow between the WE and the CE is controlled. The potential difference between the RE and WE and the current flowing between the CE and WE are continuously monitored. By using a potentiostat/galvanostat, the value specified by the user (i.e. applied potential or current) is accurately controlled, anytime during the measurement by using a negative feedback mechanism. During the electrochemical reaction (in a solution), the equilibrium concentration of the reduced and oxidized forms of a redox couple are linked to the potential (E) via Nernst's equation (5.1)

$$E = E_0 + \frac{RT}{nF} ln \frac{c_{oxi}}{c_{red}} \qquad \text{(Eq. 5.1)}$$

Where E_0 is equilibrium potential, F is Faraday's constant, T is absolute temperature,c_{oxi} and c_{red} is concentrations of oxidation and reduction centers. For each redox couple, there is a

standard potential (Eo) at which the reduced and oxidized forms are Present in equal concentration. If the potential E is applied to the working electrode with respect to the reference electrode, the redox couples present at the electrode respond to this change and adjust their concentration ratios according to (Eq. 5.1)

We used differential pulse voltammetry, cyclic voltammetry, and electrochemical impedance spectroscopy (EIS) techniques for the electrochemical characterization of different electrode GGH, APTES/MoO3, APTES/MoO3@GGH, anti-HER-2/APTES/MoO3@GGH, BSA/anti-HER-2/APTES/MoO3@GGH

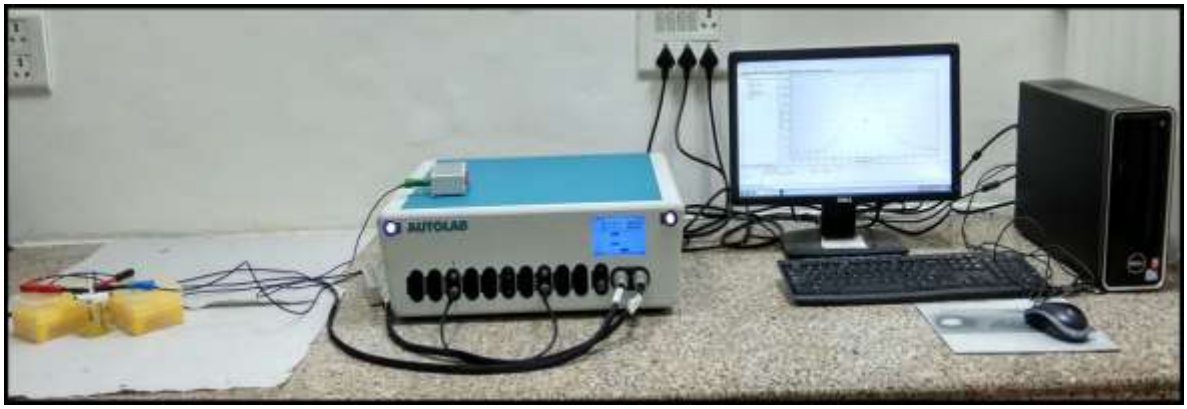

Figure 5.5: Electrochemical analyser/Autolab instrument.

CHAPTER 6

RESULTS AND DISCUSSION

6. Results and Discussion

6.1. Fourier transform infrared spectroscopy (FT-IR) studies

In the figure (6.1) GGH curve represents the peak at 3444.4 cm-1 due to N-H stretching. The sharp peak obserbed at 1651 cm^{-1} is of amide group because it present in the Ehtylenediamne [46].The other peaks at 1385.5, 1031.8, 793.6 cm^{-1} is due to the symmetrical deformations of -CH_2 group, - CH_2 twisting vibration at peak,(1–4),(1–6) linkageofgalactose and mannose, respectively [47]. In this figure (6.1) The broad band at 3428.1 cm^{-1} can be refereed as N-H stretching vibration and the band around 1618.3 assigned amide group [48]. The band at 1046.2 cm^{-1} were assirned to si-o stretching vibration of aptes to the surface of MoO_3 nanoparticles. Two additional broad peaks at 885.7 cm^{-1} and 634.2 cm^{-1} are due to M=O and M-O respectively. In the same figure (6.1) the curve of APTES/MoO_3@GGH shows the common peak of GGG and APTES/MoO_3.

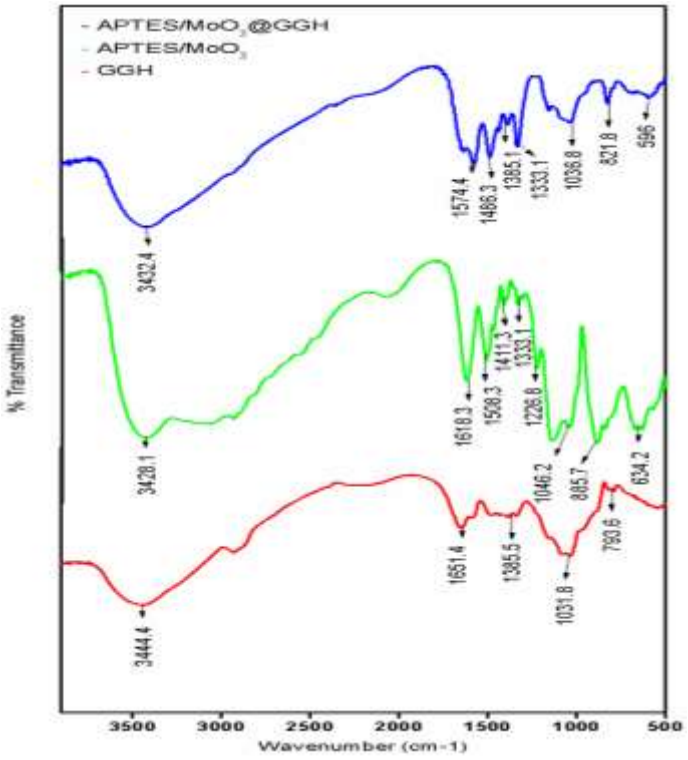

Figure 6.1: FTIR spectra of GGH, APTES/MoO_3, APTES/MoO_3@GGH

6.2. X-ray Diffraction (XRD) studies

The XRD analysis of synthesis product MoO_3 shown in above fig. The diffraction peaks corresponding to (0 0 1), ($\bar{1}$ 0 1), (0 0 2), (0 1 1), (1 0 1), (1 1 0), (0 1 2), (1 0 2), (1 1 2), (0 2 0), (1- 2 1), (0 2 2), ($\bar{1}$ 2 2) and (0 2 3) respectively planes are well matched with JCPDS NO. 85-2405. This indicates the formation of the monoclinic crystal phase of MoO_3 and no impure peak is found in the this XRD [49]. It reveals that maximum intensity and crystallites at corresponds to (0 11) The average crystallite size *"D"* has been estimated to be ≈ 10.56 nm using the Scherer formula Equation 6.1

$$D = \frac{0.9\lambda}{\beta cos\theta} \qquad \text{(Eq. 6.1)}$$

Where =1.54 Å is the wavelength of the target Cu-Kα, θ is the Bragg's diffraction angle, and beta is the full width at half maximum (FWHM) of the diffraction peak.

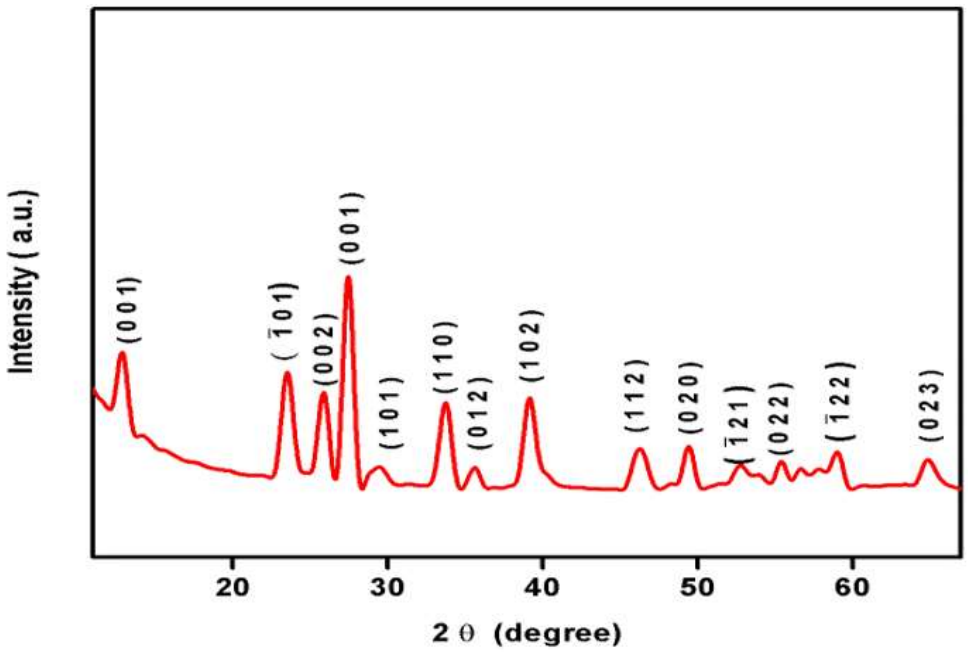

Figure 6.2: X-ray differaction of MoO_3

6.3. UV-Visible Spectrophotometer studies

We have performed the UV-Vis Spectrophotometer characterizationusing LAMBDA-950,Perkin Elmer to conform the nanocomposite hydrogel and guar gum hydrogel. The UV spectrophotometer shows the peak of GGH solution at 271 nm and nanocomposite hydrogel or APTES/MoO_3@GGH solution at 227 nm. GGH showed the maximum transparency, greater than those of the APTES/MoO_3@GGH, in the UV region because nanostructured functionalised molybdenum trioxide present in it. This may be due to the monoclinic structure of MoO_3. The blend was found to act as a barrier to block the UV-Visible rays at shorter ranges of wavelength (200–250 nm) [50].

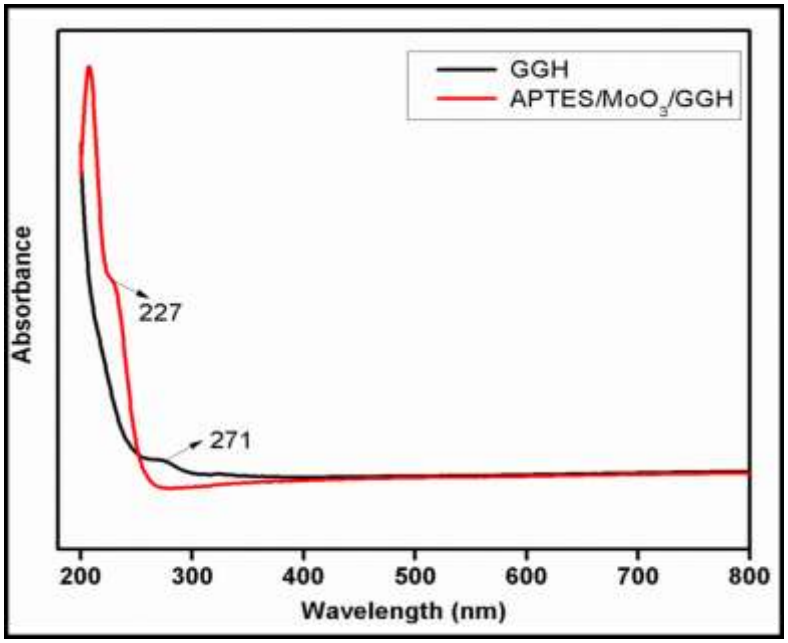

Figure 6.3: shows the UV-Visible absorption spectra of the GGH and APTES/MoO_3@GGH blend in the wavelength range of 200 –300 nm.

6.4. pH Studies

Electrochemical response of the BSA/anti-HER-2/APTES/MoO_3@GGH/ITO immunoelectrode using Differential pulse voltammetry (DPV) technique at different pH (6, 6.5, 7, 7.4 and 8) was carried out at the scan rate 50 mV/s in phosphate buffer saline (PBS)

containing 5mM $[Fe(CN)_6]^{3-/4-}$. DPV shows maximum peak current at pH 7.4 [51]. The structure of biomolecules is preserved. In acidic and basic medium pH biomolecules structure is start to denature and behaviors of the biomolecules also start changing. Thus PBS buffer with pH 7.4 was used for the electrochemical studies

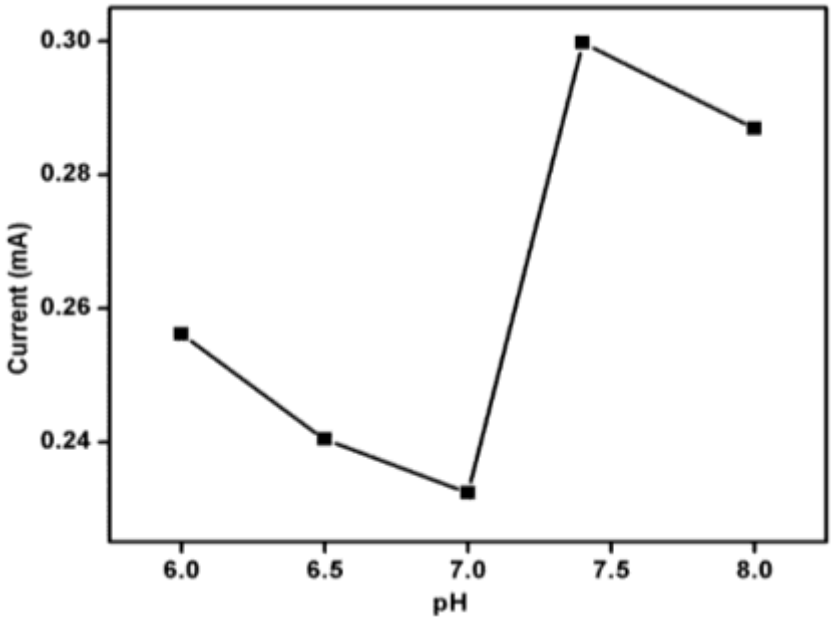

Figure 6.4: pH response of BSA/anti-HER-2/APTES/MoO_3@GGH/ITO

6.5. Electrode Studies

Differential pulse voltammetry (DPV) studies were conducted to characterize the fabricated electrode of GGH/ITO, APTES/MoO_3@GGH/ITO, anti-HER-2/APTES/MoO_3@GGH/ITO, BSA/anti-HER-2/APTES/MoO_3@GGH/ITO electrode determined in the potential range from 0.2 to 0.6 V were conducted in PBS buffer (50 mM, 0.9%NaCl) containing 5mM $[Fe(CN)_6]^{3-/4-}$ Figure 6.5 The magnitude peak current of GGH/ITO was found to be 0.1975 mA, after incorporation of APTES/MoO_3 in GGH the peak current of APTES/MoO_3@GGH/ITO increased 0.3318 mA this may be due to the the highly conducting behaviour of of MoO_3 that may have entrapped in the GGH. After the immobization of anti-HER-2 on APTES/MoO_3@GGH/ITO then peak current is found to be reduced to 0.292 mA . this

reduction in peak current may be attributed to the insulating behaviou of antibodies, which furthe obstructs the electron transfer to the electrode surface. Finally, BSA was used to block the nonspecific binding sites of anti-HER-2/APTES/MoO_3@GGH/ITO electrode . The magnitude peaks current of BSA/anti-HER-2/APTES/MoO_3@GGH/ITO electrode was found to be further reduced to 0.259 mA, reflecting the insulating characteristics of the BSA molecules [52].

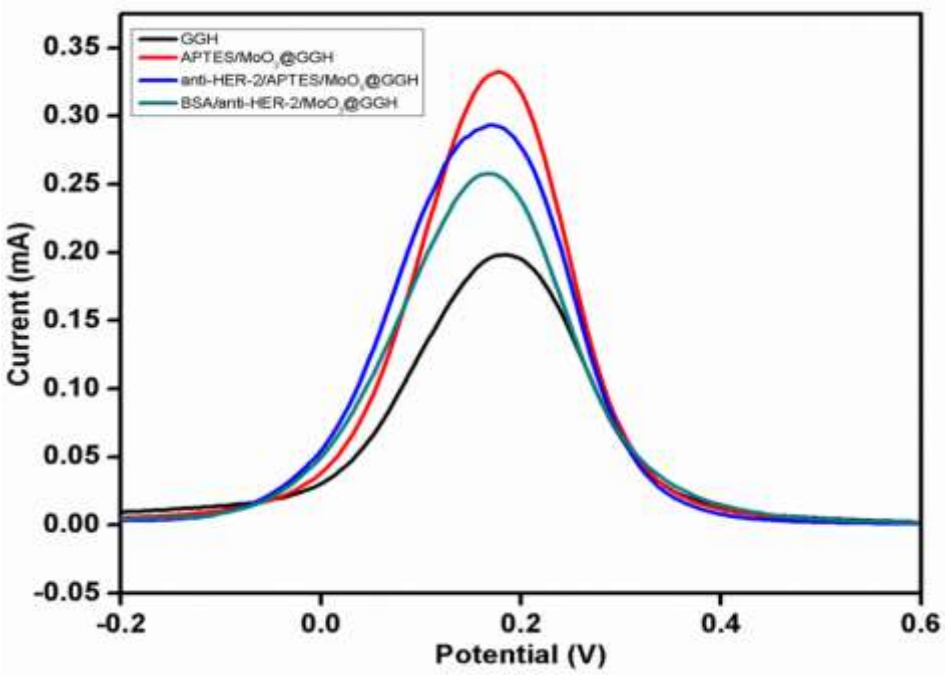

Figure 6.5: Electrode studies of GGH/ITO, APTES/MoO_3@GGH/ITO, anti-HER 2/APTES/MoO_3@GGH/ITO, BSA/anti-HER-2/APTES/MoO_3@GGH/ITO

6.6. Incubation Studies

The incubation study of BSA/anti-HER-2/APTES/MoO_3@GGH/ITO immunoelectrode using DPV technique. This shows that the intraction time between HER-2 (antigen) and antibody binding on the BSA/anti-HER-2/APTES/MoO_3@GGH/ITO immunoelectrode is upto (0-40 min) after that there is no significant change occurs or it may reaches to the stedy state.

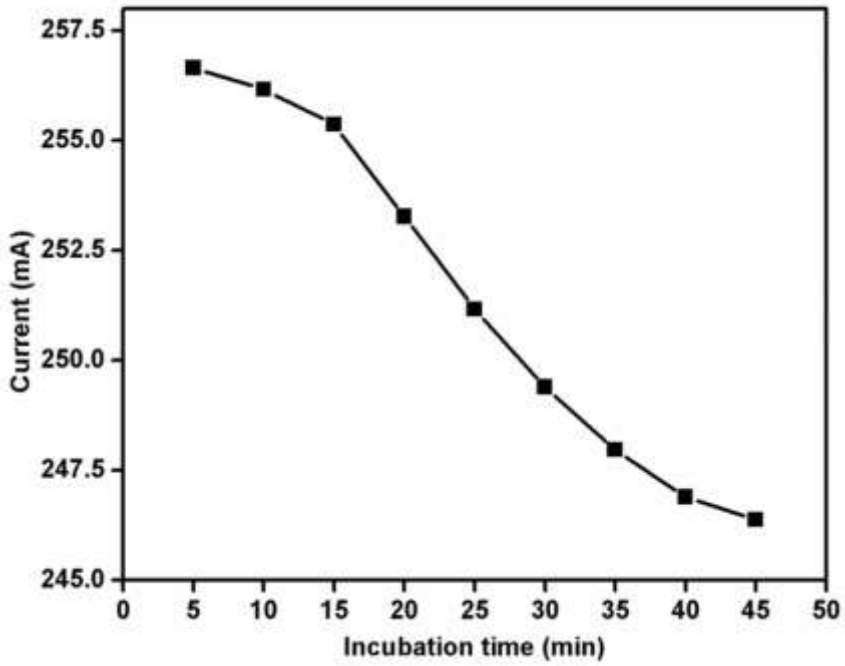

Figure 6.6: The incubation time study of interaction between HER-2 and BSA/anti-HER-2/APTES/MoO_3@GGH/ITO immunoelectrode.

6.7. Scan Rate Studies

The cyclic voltammetry (CV) of APTES/MoO_3@GGH/ITO and BSA/anti-HER-2/APTES/MoO_3@GGH/ITO electrodes were recorded as a function of scan rate (20–200mV/s) (Figure 6.7 and 6.8). The magnitudes of both anodic (I_{pa}) and cathodic (I_{pc}) peak currents exhibited a linear relationship with [scan rate (mV/s)]$^{1/2}$ has been shown in Inset (i) of (Figure 6.7 and 6.8) indicating that the electrochemical reaction is a diffusion- controlled process [53]. Intercept and slope is given by equation (6.2 - 6.5)

$\mathbf{I_{pa}}$(BSA/anti-HER-2/APTES/MoO3@GGH/ITO)

$$= [\ 0.43 \times 10^{-6}\text{A(s/mV)} \times (\text{scan rate [mV/s]})^{1/2}] + 0.01434\times10^{-6}\ \text{A} \qquad \text{(Eq. 6.2)}$$

$$R^2 = 0.993,\ SD = 8.50\times10^{-7}$$

$\mathbf{I_{pc}}$(BSA/anti-HER-2/APTES/MoO_3@GGH/ITO)

$$= -[\ 0.33 \times 10^{-6}\text{A(s/mV)} \times (\text{scan rate [mV/s]})^{1/2}] - 0.01077\times10^{-6}\ \text{A} \qquad \text{(Eq. 6.3)}$$

$$R^2 = 0.984,\ SD = 9.66\times10^{-7}$$

$\mathbf{I_{pa}}$(APTES/MoO@/GGH/ITO)

$$= [\ 0.01 \times 10^{-6}\text{A(s/mV)} \times (\text{scan rate [mV/s]})^{1/2}] + 0.0211\times10^{-6}\ \text{A} \qquad \text{(Eq. 6.4)}$$

$$R^2 = 0.994,\ SD = 0.175\times10^{-7}$$

$\mathbf{I_{pc}}$(APTES/MoO3/GGH/ITO)

$$= -[\ 0.917 \times 10^{-6}\text{A(s/mV)} \times (\text{scan rate [mV/s]})^{1/2}] - 0.0126\times10^{-6}\ \text{A} \qquad \text{(Eq. 6.5)}$$

$$R^2 = 0.993,\ SD = 0.177\times10^{-7}$$

Further, it is observed that with increasing scan rate, the oxidation peak shifts towards higher potential and the reduction peak shifts towards lower potential. The linearity is obtained between the difference in magnitude of the oxidation peak potential and reduction peak

potential (ΔE)= E_{pa} -E_{pc}, Epa is anodic peak potential, and Epc is cathodic peak potential. (ΔE) exhibited a linear relationship with [scan rate (mV/s)]$^{1/2}$ has been shown in Inset (ii) of (Figure 6.7 and 6.8) indicating smooth electrone transfer kinetics between medium to electrode [54]. and follows Equations (6.6) and (6.7) :

ΔE$_{(APTES/MoO3/\ GGH/ITO)}$

$$= [\ 21.67 \times 10^{-3}V\ (s/mV) \times (\text{scan rate } [mV/s])^{1/2}] + 0.1086\ V \qquad \text{(Eq. 6.6)}$$

$$R^2 = 0.995,\ SD = 3.45\times10^{-4}$$

ΔE$_{(BSA/anti\text{-}HER\text{-}2/APTES/MoO3/\ GGH/ITO)}$

$$= [\ 16.4 \times 10^{-3}V\ (s/mV) \times (\text{scan rate } [mV/s])^{1/2}] + 0.0932\ V \qquad \text{(Eq. 6.7)}$$

$$R^2 = 0.995,\ SD = 2.46\times10^{-4}$$

where R is the regression coefficient, and SD is the standard deviation. The diffusion coefficient (D) of BSA/anti-HER-2/APTES/MoO_3@GGH/ITO immunoelectrode has been calculated to be 3.64×10^{-11} $cm^2\ s^{-1}$ by using randle sevick equation.

$$I_P = (2.69 \times 10^5)\, n^{3/2} A D^{1/2}\, C \nu^{1/2} \qquad \text{(Eq.6.8)}$$

Where I_P is the peak current of the BSA/anti-HER-2/APTES/MoO_3@GGH/ITO immunoelectrode, A is the active surface of the immunoelectrode (0.25 cm^2), C is the concentration of the redox species (5×10^{-3} mol cm^{-2}), ν is the scan rate (50 mV/s). By using Laviron's theory surface concentration has been calculated to be 3.857×10^{-8} mol cm^{-2} BSA/anti-HER-2/APTES/MoO_3@GGH/ITO immunoelectrode.

$$I_P = n^2 F^2\, \gamma A \nu (4RT)^{-1} \qquad \text{(Eq.6.9)}$$

Where I_P is the peak current of the BSA/anti-HER-2/APTES/MoO_3@GGH/ITO immunoelectrode, n is the number odf electron (1) transferred, F is the Faraday constant (96485.322 C mol^{-1}), γ is the surface concentration of the absorbed electro- active species,Ais

the surface area of the electrode, ν is the scan rate (50 mV/s), R is the the molar gas constant (8.314 J mol^{-1} K^{-1}), T is the room temperature (25 ºC or 298K)

To find the heterogeneous electron transfer (HET) of GGH/ITO and APTES/MoO_3@GGH/ITO electrochemical impedance spectoscopy (EIS) were performed at at 50 mV/s. The HET (0.745×10^{-7} cm s^{-1}) of GGH/ITO electroe is found to increase upto four times (3.094×10^{-7} cm s^{-1}) when APTES/MoO_3 is incorporated in APTES/MoO_3@GGH/ITO electrode facilitating faster electron transfer.

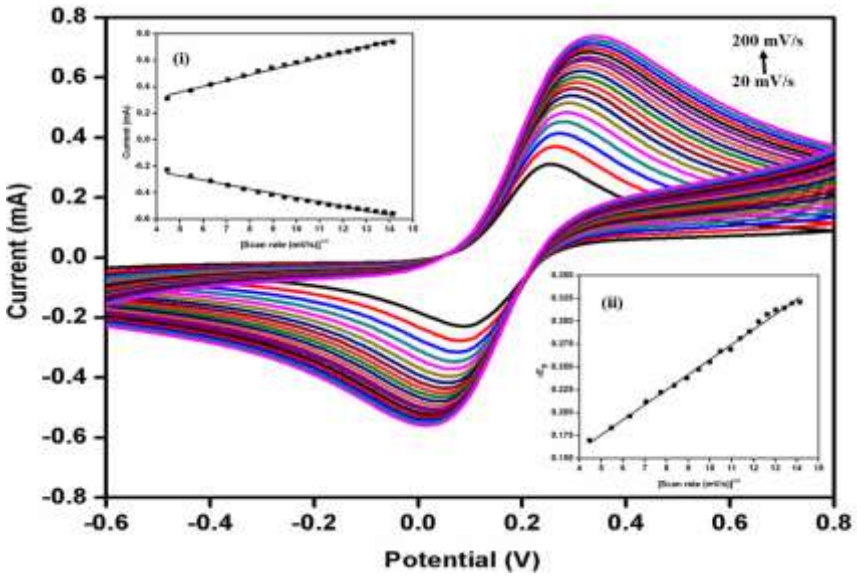

Figure 6.7: Scan rate studis using CV of BSA/anti-HER-2/APTES/MoO_3@GGH/ITO electrode as a function of scan rate (20 – 200 mV/s) Inset (i) magnitude of anodic (I_{pa}) and cathodic (I_{pc}) peak current as a function of scan rate (mV/s), Inset (ii) Difference potential $\Delta E_p = E_{pa} - E_{pc}$ as a function of scan rate.

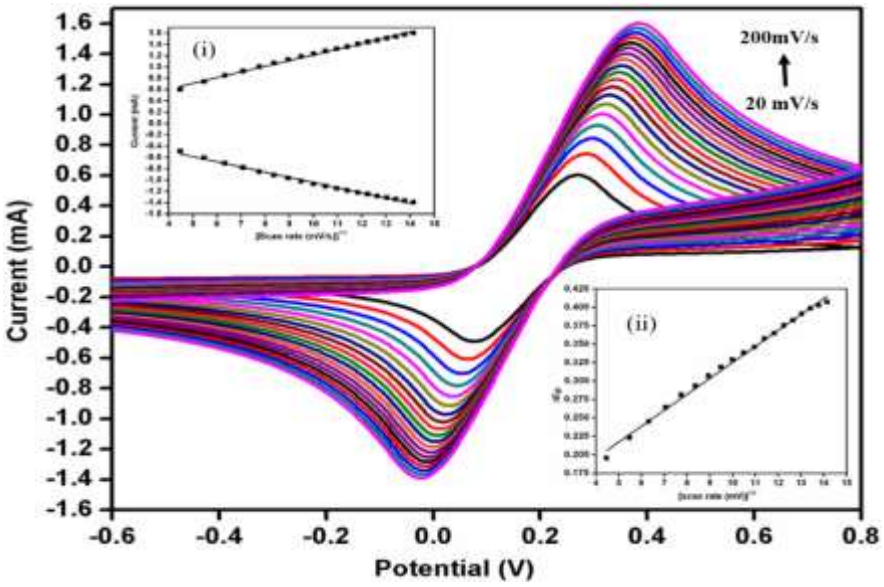

Figure 6.8: Scan rate studies using CV of APTES/MoO_3@GGH/ITO electrode as a function of scan rate (20 – 200 mV/s) Inset (i) magnitude of anodic (I_{pa}) and cathodic (I_{pc}) peak current as afunction of scan rate (mV/s), Inset (ii) Difference potential $\Delta E_p = E_{pa} - E_{pc}$ as a function of scan rate.

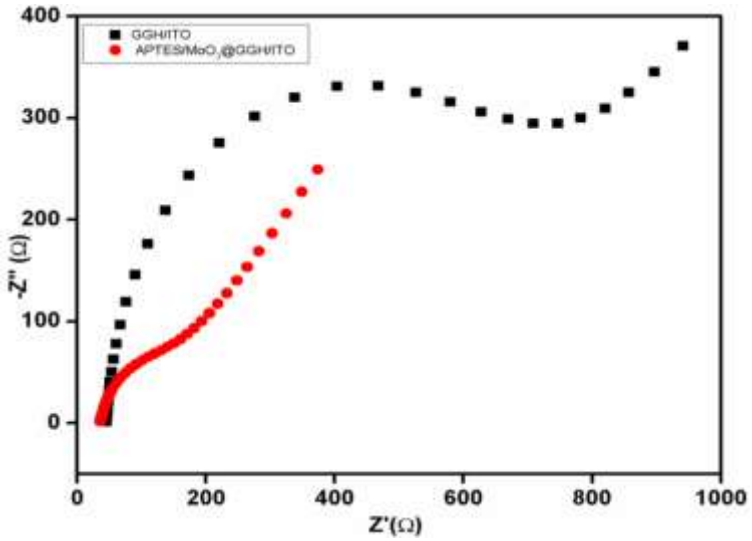

Figure 6.9: shows that the heterogeneous electron transfer (HET) of GGH/ITO and APTES/MoO_3@GGH/ITO electrochemical impedance spectroscopy (EIS) were performed at 50 mV/s.

6.8. Electrochemical response Studies

The electrochemical response study of BSA/anti-HER-2/APTES/MoO_3@GGH/ITO immunoelectrode determined as a function of concentration (1fg mL^{-1} – 10^3 ng mL^{-1}) is shown in figure 6.10. The experiments were conducted in PBS buffer (50 mM, 0.9%NaCl) containing $[Fe(CN)_6]^{3-/4-}$ (5 mM) at a scan rate of 50 mV s^{-1} in the potential range, - 0.2 to 0.6V using DPV technique. The immunoelectrode was incubated with antigen solution for 30 min for antigen-antibody interaction before the DPV measurements. It was found that the electrochemical peak current gradually decreased linearly with increased concentration of HER2 inset (i) in Figure (6.10) [55]. The reduced current is attributed to the formation of an electrically insulating antigen-antibody complex that perhaps obstructs the electron transfer through $[Fe(CN)_6]^{3-/4-}$. The observed calibration curve between peak current and antigen concentration obeys equation (6.10)

$$\mathbf{I_P} = - [3.01605 \times 10^{-6} \times \text{concentration of HER 2 [1fg mL}^{-1} – 10^3 \text{ ng mL}^{-1}] – 0.024 \times 10^{-6}]$$

$$R^2 = 0.978 \qquad \text{(Eq.6.10)}$$

Figure 6.10 inset (iii) reveals that linearity is obtained in the range, [1fg mL^{-1} – 10^3 ng mL^{-1}], sensitivity is 12.28 µA mL $ng^{-1}cm^{-2}$ with regression coefficient (R^2) of 0.978, and the lower detection limit is 0.13249 ng mL^{-1}. The limit of detection is calculated using the standard equation (6.11)

$$\text{Limit of detection} = 3\ \sigma/\text{Sensitivity} \qquad \text{(Eq.6.11)}$$

where σ is the standard deviation of the BSA/anti-HER-2/APTES/MoO_3@GGH/ITO immunoelectrode.

We conducted a control experiment to investigate the electrochemical response of APTES/MoO_3@GGH/ITO electrode towards HER-2 without using anti-HER-2 in figure (6.10) inset (iv). We did not observe any significant changes in the magnitude of the peak current on different concentration of HER-2. This result indicates that the sensor response is likely to be due to the immunoreaction between anti-HER-2and HER-2 molecules.

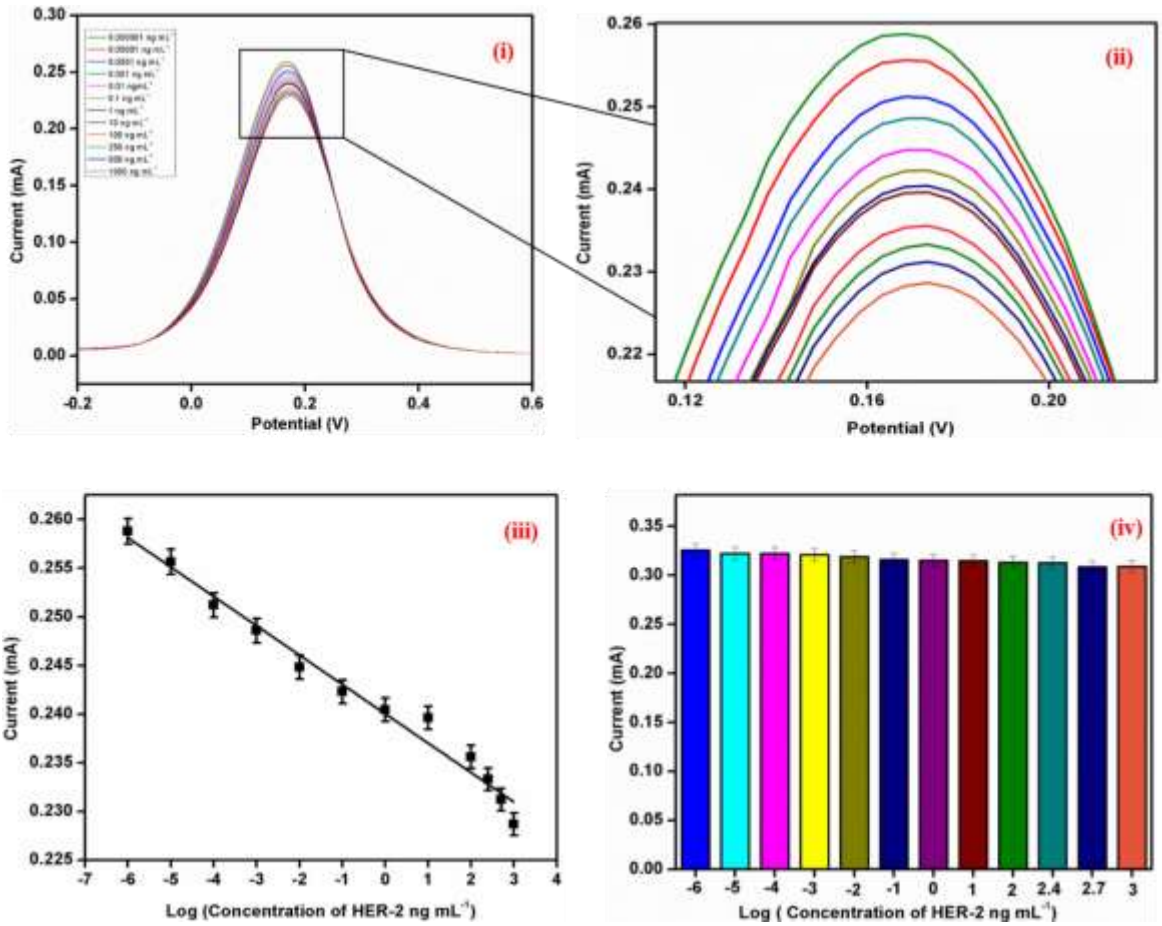

Figure 6.10: (i) Electrochemical response studies of BSA/anti-HER-2/APT ES/MoO_3@GGH/ITO immunoelectrode as a function of HER-2 concentration(1fg mL^{-1} – 10^3 ng mL^{-1}) (ii) Magnified view of peak current (iii) Calibration curve between peak current magnitude and HER-2 concentration (iv) Control studies of BSA/anti-HER-2/APT ES/MoO_3@GGH/ITO immunoelectrode as a function of HER-2 concentration (1fg mL^{-1} – 10^3 ng mL^{-1})

6.9. Interferent Studies

Interferent studies Figure 6.11 of fabricated BSA/anti-HER-2/APTES/MoO_3@GGH/ITO immunoelectrode has been performed through DPV by incubating it with different interfering analytes supposed to present in human serum such as glucose (mg mL^{-1}), endotheline-1(10^5 pg mL^{-1}), carcino embryonic antigen (CEA) (500 ng mL^{-1}), cTnI (500ng mL^{-1}), CYFRA-21-1(2 ng mL^{-1}), HER-2 (10^3 ng mL-1) etc. We observed that there is no significant change in magnitude of peak current on the addition of different analytes. This indicate the high selectivity of fabricated BSA/anti-HER-2/APTES/MoO_3@GGH/ITO immunoelectrode for detection of HER-2 antigen.

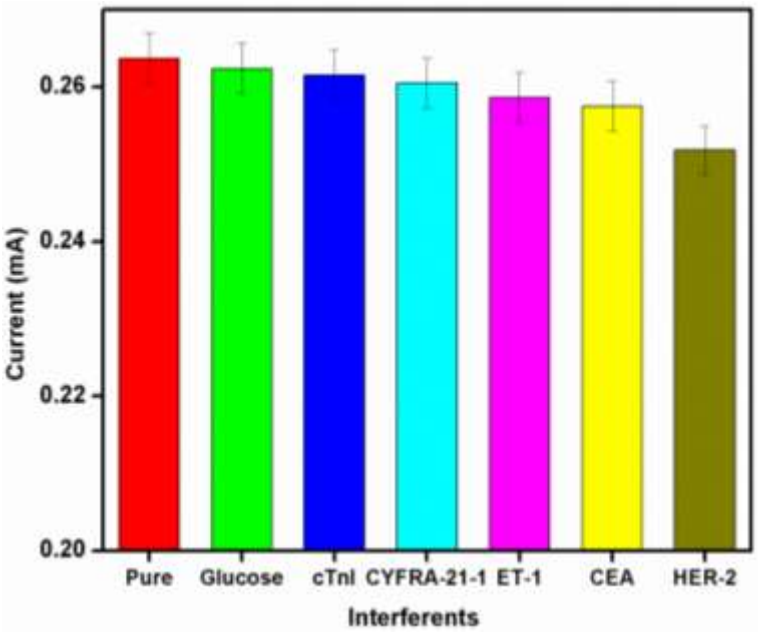

Figure 6.11: Interferent studies of fabricated BSA/anti-HER-2/APTES/MoO_3 /GGH/ITO immunoelectrode

6.10. Shelf Life Studies

The shelf life study of fabricated BSA/anti-HER-2/APTES/MoO_3@GGH/ITO immunoelectrode has been observed by measuring the change in magnitude of peak current at regular intervals in a standard solution of HER-2 in PBS at the one-week interval for about four weeks. Immunoelectrode is stored at 4 º C when not in use.

Table 1

Various detection technique used for breast cancer detection

Method	Detection technique	Label	Sample	Biomarker	Platform	Conteration Range of biomarker	Linear detection range	Senstivity	Response time	Lower detection limit	Reference
FISH	optical	yes	Tissue						48 hours		[56]
IHC	staining	yes	tissue						48 hours		[57]
ELISA	Plate-based assay	No	serum	HER-2 ECD		> 2 ng mL^{-1}	0 – 3 ng mL^{-1}			0.123 ng mL^{-1}	[58]
Biosensor	Acoustic	No	Serum	HER-2/neu		2 - 75 ng mL^{-1}	13-20 ng mL^{-1}				[59]
	Electrochemical (DPV)	No	serum	HER-2	Hyd-AuNP-Apt/HER2/anti-HER2/poly-DPB-(AuNP)/GC	2 - 75 ng mL^{-1}	1 pg mL^{-1} – 10 ng mL^{-1}	1.117±0.008 µA mL ng^{-1}		0.037±0.002 pg mL^{-1}	[60]
	piezoelectric microcantilevers	No	serum	HER-2 ECD		> 2 ng mL^{-1}	0.005-2 ng mL^{-1}		90 min	0.0253 ng mL^{-1}	[58]
	Opto-fludic ring resonator	No	serum	HER-2		2 - 75 ng mL^{-1}	13-30 ng mL^{-1}		30 min		[61]
	Electrochemical (DPV)	No	serum	HER-2	BSA/anti-HER2/Aptes/MoO_3@GGH/ITO	2 - 75 ng mL^{-1}	1 fg mL^{-1} – 1000 ng mL^{-1}	3.01605 µA mL ng^{-1}	30 min	0.132 ng mL^{-1}	Present work

CHAPTER 7

CONCLUSION

7. Conclusion

We have fabricated a simple, high sensitive, label-free, MoO_3 incorporated guar gum hydrogel based biosensing platform for breast detection. MoO_3 nanoparticles have been synthesized via the hydrothermal method, and its functionalization has been achieved using APTES. Thin films of APTES/ MoO_3@GGH/ITO have been fabricated via drop cast and followed by, covalent immobilization of antibodies. The HER-2 antigen has been used as a biomarker for the detection of breast cancer. In comparison with other reported breast cancer detection methods including biosensors, the BSA/anti- HER2/APTES/ MoO_3@GGH/ITO biosensor is simple, exhibits a wider detection range of 1fg – 10^3 ng mL −1 high sensitivity of 3.01 mA mL ng $^{-1}$, detection limit of 0.132 ng mL $^{-1}$, and shelf-life of four weeks. This novel serum based breast cancer biomarker (HER-2) opens a new window for research in breast and other cancers.

CHAPTER 8

FUTURE PERSPECTIVES

8. Future perspectives

The present experiment is found to reveals that the APTES/ MoO_3@GGH platform can efficiently be utilized in the development of sensitive and high-performance electrochemical biosensing devices for point of care applications, detection, and prognosis of diseases. To further increase the stability and sensitivity of this fabricated efforts should be made.

CHAPTER 9
REFRENCES

9. References

1. Maitra, Jaya, and Vivek Kumar Shukla. "Cross-linking in hydrogels-a review." *American Journal of Polymer Science* 4.2 (2014): 25-31.
2. Billiet, T.; Vandenhaute, M.; Schelfhout, J.; van Vlierberghe, S.; Dubruel, P. A review of trends and limitations in hydrogel-rapid prototyping for tissue engineering. *Biomaterials* 2012, *33*, 6020–6041
3. Hoffman, A.S. Hydrogels for biomedical applications. *Adv. Drug Deliv. Rev.* 2012, *64*, 18–23.
4. Lin, Jianming, Qunwei Tang, and Jihuai Wu. "The synthesis and electrical conductivity of a polyacrylamide/Cu conducting hydrogel." *Reactive and Functional Polymers* 67.6 (2007): 489-494.
5. Anseth, Kristi S., Christopher N. Bowman, and Lisa Brannon-Peppas. "Mechanical properties of hydrogels and their experimental determination." *Biomaterials* 17.17 (1996): 1647-1657.
6. Patel, Alpesh, and Kibret Mequanint. "Hydrogel biomaterials." *Biomedical engineering-frontiers and challenges*. InTech, 2011.
7. Bahram, Morteza, Naimeh Mohseni, and Mehdi Moghtader. "An Introduction to Hydrogels and Some Recent Applications." *Emerging Concepts in Analysis and Applications of Hydrogels*. InTech, 2016.
8. Zhao, Yu, et al. "3D nanostructured conductive polymer hydrogels for high-performance electrochemical devices." *Energy & Environmental Science* 6.10 (2013): 2856-2870.
9. Et al Li, Lanlan, et al. "A nanostructured conductive hydrogels-based biosensor platform for human metabolite detection." *Nano letters* 15.2 (2015): 1146-1151.

10. Qu, Fengli, et al. "Electrochemical biosensing platform using hydrogel prepared from ferrocene modified amino acid as highly efficient immobilization matrix." *Analytical chemistry* 86.2 (2014): 973-976.
11. Rong, Qinfeng, et al. "Network nanostructured polypyrrole hydrogel/Au composites as enhanced electrochemical biosensing platform." *Scientific reports* 5 (2015): srep11440.
12. Slamon, Dennis J., et al. "Use of chemotherapy plus a monoclonal antibody against HER2 for metastatic breast cancer that overexpresses HER2." *New England Journal of Medicine* 344.11 (2001): 783-792.
13. Arkan, Elham, et al. "A novel antibody–antigen based impedimetric immunosensor for low level detection of HER2 in serum samples of breast cancer patients via modification of a gold nanoparticles decorated multiwall carbon nanotube-ionic liquid electrode." *Analytica chimica acta* 874 (2015): 66-74.
14. Ahmed, Enas M. "Hydrogel: Preparation, characterization, and applications: A review." *Journal of advanced research* 6.2 (2015): 105-121.
15. Santhi priya. Nagam*, a. Naga jyothi, j. Poojitha, santhosh aruna, rama rao nadendla , a comprehensive review on hydrogels, *International Journal of Current Pharmaceutical Research 2015.*
16. Chen, Gang, Yujia Wang, and Jin-Long Huang. "Breast cancer following polyacrylamide hydrogel injection for breast augmentation: A case report." *Molecular and clinical oncology* 4.3 (2016): 433-435.
17. Das, Aditi, Saurabh Wadhwa, and A. K. Srivastava. "Cross-linked guar gum hydrogel discs for colon-specific delivery of ibuprofen: formulation and in vitro evaluation." *Drug delivery* 13.2 (2006): 139-142.

18. Gryadunov, Dmitry, et al. "Gel-based microarrays in clinical diagnostics in Russia." *Expert review of molecular diagnostics* 11.8 (2011): 839-853.
19. Huang, Yihong, Huiqun Yu, and Chaobo Xiao. "pH-sensitive cationic guar gum/poly (acrylic acid) polyelectrolyte hydrogels: Swelling and in vitro drug release." *Carbohydrate Polymers* 69.4 (2007): 774-783.
20. Li Yuhui, Huang Guoyou, Zhang Xiaohui, Li Baoqiang, Chen Yongmei, Lu Tingli, Lu Tian Jian, Xu Feng. Magnetic hydrogels and their potential biomedical applications. AdvFunct Mater 2013;23(6):660–72.
21. Ahmed, Enas M. "Hydrogel: Preparation, characterization, and applications: A review." *Journal of advanced research* 6.2 (2015): 105-121.
22. Burkert, Sina, et al. "Cross-linking of poly (N-vinyl pyrrolidone) films by electron beam irradiation." *Radiation Physics and Chemistry* 76.8 (2007): 1324-1328.
23. Hachem, Ray, et al. "Novel antiseptic urinary catheters for prevention of urinary tract infections: correlation of in vivo and in vitro test results." *Antimicrobial agents and chemotherapy* 53.12 (2009): 5145-5149.
24. Kumar, Suveen, et al. "Biofunctionalized nanostructured zirconia for biomedical application: a smart approach for oral cancer detection." *Advanced Science* 2.8 (2015).
25. Horie, Masanori, et al. "Protein adsorption of ultrafine metal oxide and its influence on cytotoxicity toward cultured cells." *Chemical research in toxicology* 22.3 (2009): 543-553.
26. Tevet, O., et al. "Nanocompression of individual multilayered polyhedral nanoparticles." *Nanotechnology* 21.36 (2010): 365705.
27. Ansari, Anees A., Pratima R. Solanki, and B. D. Malhotra. "Sol-gel derived nanostructured cerium oxide film for glucose sensor." *Applied Physics Letters* 92.26 (2008): 263901.

28. Choi, Han Nim, Min Ah Kim, and Won-Yong Lee. "Amperometric glucose biosensor based on sol–gel-derived metal oxide/Nafion composite films." *Analytica chimica acta* 537.1 (2005): 179-187.
29. Singh, S. P., et al. "Cholesterol biosensor based on rf sputtered zinc oxide nanoporous thin film." *Applied Physics Letters* 91.6 (2007): 063901.
30. Solanki, Pratima R., et al. "Nanostructured metal oxide-based biosensors." *NPG Asia Materials* 3.1 (2011): 17-24.
31. Vigneshvar, S., et al. "Recent advances in biosensor technology for potential applications–an overview." *Frontiers in bioengineering and biotechnology* 4 (2016).
32. Grieshaber, Dorothee, et al. "Electrochemical biosensors-sensor principles and architectures." *Sensors* 8.3 (2008): 1400-1458.
33. Zhang, J. X., et al. "Large field-induced strains in a lead-free piezoelectric material." *Nature Nanotechnology* 6.2 (2011): 98-102.
34. Hejmadi, Momna. *Introduction to cancer biology*. Bookboon, 2009.
35. Fisher, Bernard, et al. "Tamoxifen for prevention of breast cancer: report of the National Surgical Adjuvant Breast and Bowel Project P-1 Study." *JNCI: Journal of the National Cancer Institute* 90.18 (1998): 1371-1388.
36. Yager, James D., and Nancy E. Davidson. "Estrogen carcinogenesis in breast cancer." *New England Journal of Medicine* 354.3 (2006): 270-282.
37. Andreea, Gheonea Ioana, et al. "The role of imaging techniques in diagnosis of breast cancer." *J. Curr. Health Sci* 37.2 (2011): 241-248.
38. Perez, Edith A., et al. "HER2 testing in patients with breast cancer: poor correlation between weak positivity by immunohistochemistry and gene amplification by fluorescence in situ hybridization." *Mayo Clinic Proceedings*. Vol. 77. No. 2. Elsevier, 2002.

39. Ramos-Vara, J. A., and M. A. Miller. "When tissue antigens and antibodies get along: revisiting the technical aspects of immunohistochemistry—the red, brown, and blue technique." *Veterinary pathology* 51.1 (2014): 42-87.
40. Murali, Ragothaman, Ponraj Vidhya, and Palanisamy Thanikaivelan. "Thermoresponsive magnetic nanoparticle–aminated guar gum hydrogel system for sustained release of doxorubicin hydrochloride." *Carbohydrate polymers* 110 (2014): 440-445.
41. Lewis, Ian R., and Howell Edwards. *Handbook of Raman spectroscopy: from the research laboratory to the process line*. CRC Press, 2001.
42. Perkampus, Heinz-Helmut, and Heide-Charlotte Grinter. *UV-VIS Spectroscopy and its Applications*. Berlin: Springer-Verlag, 1992.
43. Wang, Hui, et al. "Sonochemical method for the preparation of bismuth sulfide nanorods." *The Journal of Physical Chemistry B* 106.15 (2002): 3848-3854.).
44. Goldstein, Joseph, ed. *Practical scanning electron microscopy: electron and ion microprobe analysis*. Springer Science & Business Media, 2012).
45. Carvalhal, Rafaela Fernanda, Renato Sanches Freire, and Lauro Tatsuo Kubota. "Polycrystalline Gold Electrodes: A Comparative Study of Pretreatment Procedures Used for Cleaning and Thiol Self-Assembly Monolayer Formation." *Electroanalysis* 17.14 (2005): 1251-1259.
46. Soppirnath, Kumaresh S., and Tejraj M. Aminabhavi. "Water transport and drug release study from cross-linked polyacrylamide grafted guar gum hydrogel microspheres for the controlled release application." *European Journal of Pharmaceutics and Biopharmaceutics* 53.1 (2002): 87-98.).

47. Mudgil, Deepak, Sheweta Barak, and B. S. Khatkar. "X-ray diffraction, IR spectroscopy and thermal characterization of partially hydrolyzed guar gum." *International journal of biological macromolecules* 50.4 (2012): 1035-1039.).
48. Bordbar, A. K., et al. "Characterization of modified magnetite nanoparticles for albumin immobilization." *Biotechnology research international* 2014 (2014).
49. Sharma, Rabindar K., and G. B. Reddy. "Synthesis and characterization of α-MoO3 microspheres packed with nanoflakes." *Journal of Physics D: Applied Physics* 47.6 (2014): 065305.).
50. Pramanik, Nilkamal, et al. "Characterization and evaluation of curcumin loaded guar gum/polyhydroxyalkanoates blend films for wound healing applications." *RSC Advances* 5.78 (2015): 63489-63501.).
51. Murali, Ragothaman, Ponraj Vidhya, and Palanisamy Thanikaivelan. "Thermoresponsive magnetic nanoparticle–aminated guar gum hydrogel system for sustained release of doxorubicin hydrochloride." *Carbohydrate polymers* 110 (2014): 440-445.)
52. Kumar, Suveen, et al. "Nanostructured zirconia decorated reduced graphene oxide based efficient biosensing platform for non-invasive oral cancer detection." *Biosensors and Bioelectronics* 78 (2016): 497-504.).
53. Vasudev, Abhay, Ajeet Kaushik, and Shekhar Bhansali. "Electrochemical immunosensor for label free epidermal growth factor receptor (EGFR) detection." *Biosensors and Bioelectronics* 39.1 (2013): 300-305.)
54. Kumar, Saurabh, et al. "Reduced graphene oxide modified smart conducting paper for cancer biosensor." *Biosensors and Bioelectronics* 73 (2015): 114-122.)

55. Kumar, Suveen, et al. "Highly sensitive protein functionalized nanostructured hafnium oxide based biosensing platform for non-invasive oral cancer detection." *Sensors and Actuators B: Chemical* 235 (2016): 1-10.
56. Salido, Marta, et al. "A comparative study of HER2/neu amplification and overexpression using fluorescencein situ hybridization (FISH) and immunohistochemistry (IHC) in 101 breast cancer patients." *Revista de Oncología* 4.5 (2002): 255-259.
57. Zaha, Dana Carmen. "Significance of immunohistochemistry in breast cancer." *World journal of clinical oncology* 5.3 (2014): 382.
58. Loo, LiNa, et al. "Highly sensitive detection of HER2 extracellular domain in the serum of breast cancer patients by piezoelectric microcantilevers." *Analytical chemistry* 83.9 (2011): 3392-3397.
59. Gruhl, Friederike J., Michael Rapp, and Kerstin Länge. "Label-free detection of breast cancer marker HER-2/neu with an acoustic biosensor." *Procedia Engineering* 5 (2010): 914-917.
60. Zhu, Ye, Pranjal Chandra, and Yoon-Bo Shim. "Ultrasensitive and selective electrochemical diagnosis of breast cancer based on a hydrazine–Au nanoparticle–aptamer bioconjugate." *Analytical chemistry* 85.2 (2012): 1058-1064.
61. Gohring, John T., Paul S. Dale, and Xudong Fan. "Detection of HER2 breast cancer biomarker using the opto-fluidic ring resonator biosensor." *Sensors and Actuators B: Chemical* 146.1 (2010): 226-230.